TWO WAVELENGTH PICOSECOND RANGING ON GROUND TARGET

K. Hamal, I. Prochazka
Faculty of Nuclear Science and Physical Engineering
Brehova 7, 11519 Prague 1 Czechoslovakia

Telephone (2) 84 8840
Telex 121254

J. Gaignebet
C.E.R.G.A.
Avenue Nicolas Copernic 06130 Grasse France

Telephone (93) 36 58 49
Telex 470865

ABSTRACT

One of the limiting factors to decrease the systematic error of laser ranging is the influence of the atmospheric refraction. Two colour ranging may contribute useful information for more precise refraction factor modelling and calculation. We describe two wavelength experiment using linear sweep streak camera for ground target distance measurement. The flight time difference 16 psec corresponding to 100 m horizontal pass was measured with RMS = 5 psec.

TWO WAVELENGTH PICOSECOND RANGING ON GROUND TARGET

The third generation of the satellite laser ranging was/1/ characterised by RMS less than 3cm, RMS below 1cm may be accepted for 4-th generation. The error budget consists in principle of the instrumental error (including timing), target error contribution and the enviromental errors.

One of the possibility to verify the existing atmospheric models, the multiwavelength laser ranging experiment, may be accomplished. The time diference (TD) in the flying time is increasing with increasing ratio of the wavelengths to be used. For this reason, the harmonic generation will be the natural choise for such an experiment. To be able to model the atmospheric refraction index with accuracy required on the basis of the TD, the TD must be measured with the accuracy of 3-7psec /2/.

Assuming the existing photocathode materials and their quantum efficiencies, two wavelength laser ranging experiment may be carried out using high power laser pulses. The available choise is ruby (1HG/2HG), Nd YAG (2HG/3HG), Alexandrite /3/ (1HG/2HG) and Emerald (1HG/2HG). Several kinds of photoreceivers may be adopted. A considerable effort was put to exploit two photomultipliers for 1km target ranging and the circular scan streak tube has been proposed /2/.

In our experiment we are using linear streak camera as a photoreceiver for ranging the 100meter target. The block scheme is on fig.1. The Nd YAG laser /4/ is used to generate the mode locked train of picosecond pulses. The Nd YAG rod 70mm/7mm is cut at 1° near the 100% mirror. The perpendicular surface on the opposite side acts as the output coupler. The saturable dye ML51 /5/ is in 2mm thin cell in contact with the 100% mirror. One milimeter apperture restrictes the laser to single transversal mode operation. The reprate is 1pps. The concentration of the dye is set to generate short train of pulses consisting of 2 or 3 pulses at FWHM of the envelope, the time interval between the pulses is 2.nsec. The output beam passes the second harmonic generator (2HG) and the third harmonic generator (3HG) using TypeII/TypeII KDP crystals. The output beam is reflected by the corner reflector at the distance 100m. The reflected light passes the ND

filters and the dispersion prism and illuminates the photocathode of the streak camera (Hammamatsu C979 /7/). The streak image is recorded by the SIT TV camera and processed in the Temporal Analyser Hammamatsu C1098. The digitalised data from the Temporal analyser are on-line transfered to the HP65 calculator (one streak window/15 seconds) for processing, statistical treatment, display, plot and storing. The data may be off-line processed on the HP1000 computer.

During the initial stage, the indoor experiment was carried out. The statistical treatment of the laser pulse length gives the value 34+/-4.5 psec at 0.53um (raw data). The histogram of pulse length is on fig.2. Assuming the 30um slit width and 4psec/channel, the deconvoluted value of the typical pulse length is 30 psec. The measured pulse length at 0.35 um is 20psec.

To obtain a smooth streak record of a pulse and hence the required time resolution, several hundreds photons are necessary. This value is consistent with the value of 570 photons published in /6/. The streak readout system permits to process two windows of one streak image simultaneously. This way, both pulses at different wavelength are recorded at the same time and thus we eleiminated the streak trigger jitter. The cross sweep streak image distorsion was testet and found to be below resclution limit. On fig.3 there is a record of the 0.53 and 0.35um signals. The time delay of in the indoor pass 6+-2psec was determined on the basis of 8 measurements (the histogram of measured values is on fig.4).

During the ground target ranging stage the corner cube retroreflector has been placed at 100 meter distance. The typical streak record at 0.53/0.35um is on fig.5. Due to a complex far field pattern structure of the 2-nd/3-rd harmonics, the two colours were not fully spatialy resolved on the streak input apperture. Totaly, 23 strak measurements were made during 20 minutes. The histogram of the measurements is on fig.6. The mean of the delay is 22psec, the RMS is 4.5psec. Refering to the indoor experiment (0.53/0.35um, TD=6+-2psec), the corrected outdoor two wavelength time delay is therefore 16psec, RMS=5psec. Taking into account the atmospheric conditions of that day, the calculated value /7/ of the 0.53/0.35um TD is 16psec. To increase the confidence of our results, more data would be perhaps necessary to obtain.

L i t e r a t u r e

1/ The Second Workshop on the Laser Tracking Instrumentation, edited by.J.Weifenbach and K.Hamal,Prague,1975

2/ J.B.Abshire, Applied Optics 19,No20,1980,3436-3440.

3/ V.N.Lisitsin et. all, Quantum Electronics,9,198, p 609,(in russian)

4/ H.Jelinkova, Mode Locked Train YAG Laser Contact Cell Preprint Series FJFI No. /64

5/ K.Hamal, to be published

6/ Picosecond Streak Camera and its Aplications, Picosecod, Vol 14, June 1983, published by Hamamatsu Corp., Japan
7/ J.W.Marini, C.W.Murray, "Correction of Laser Tracking Data for Atmospheric Refraction at Elevations Above 10 Degrees" GSFC X-591-73-351, November 1973

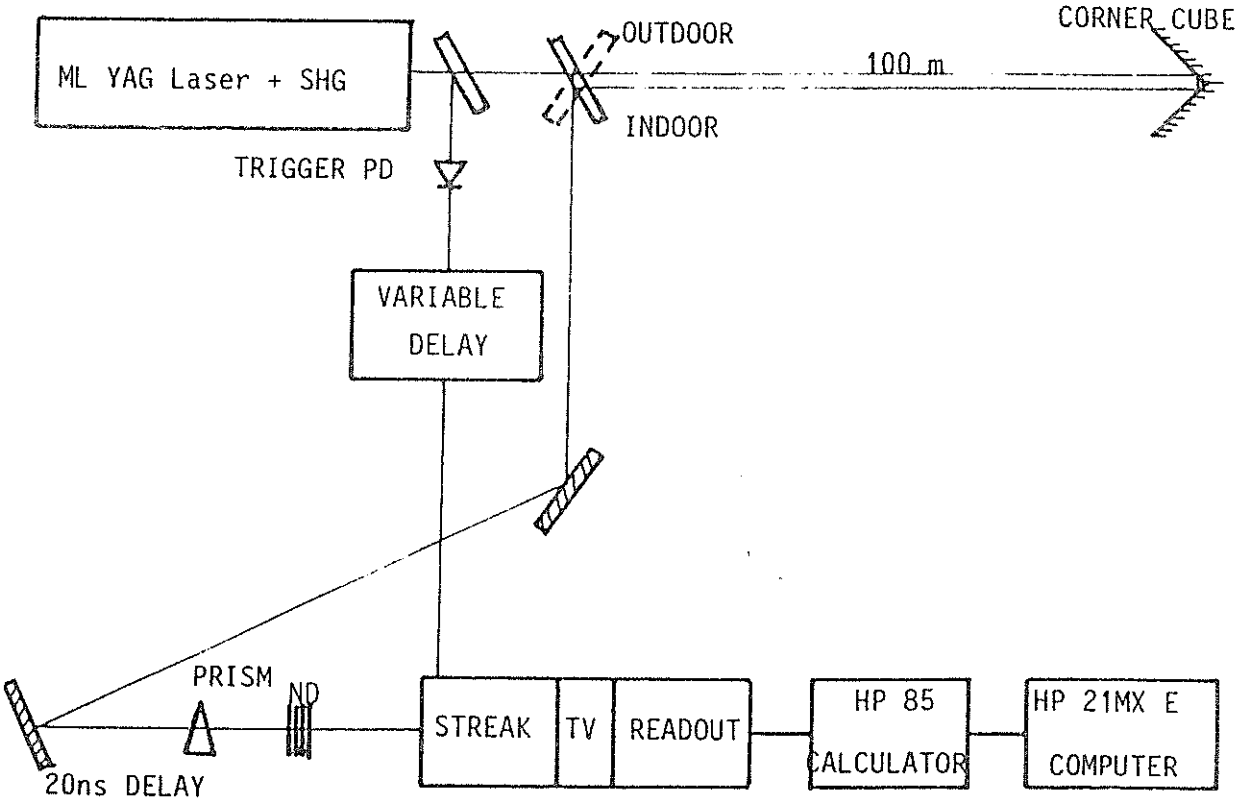

BLOCK SCHEME OF THE TWO WAVELENGTH PICOSECOND RANGING EXPERIMENT

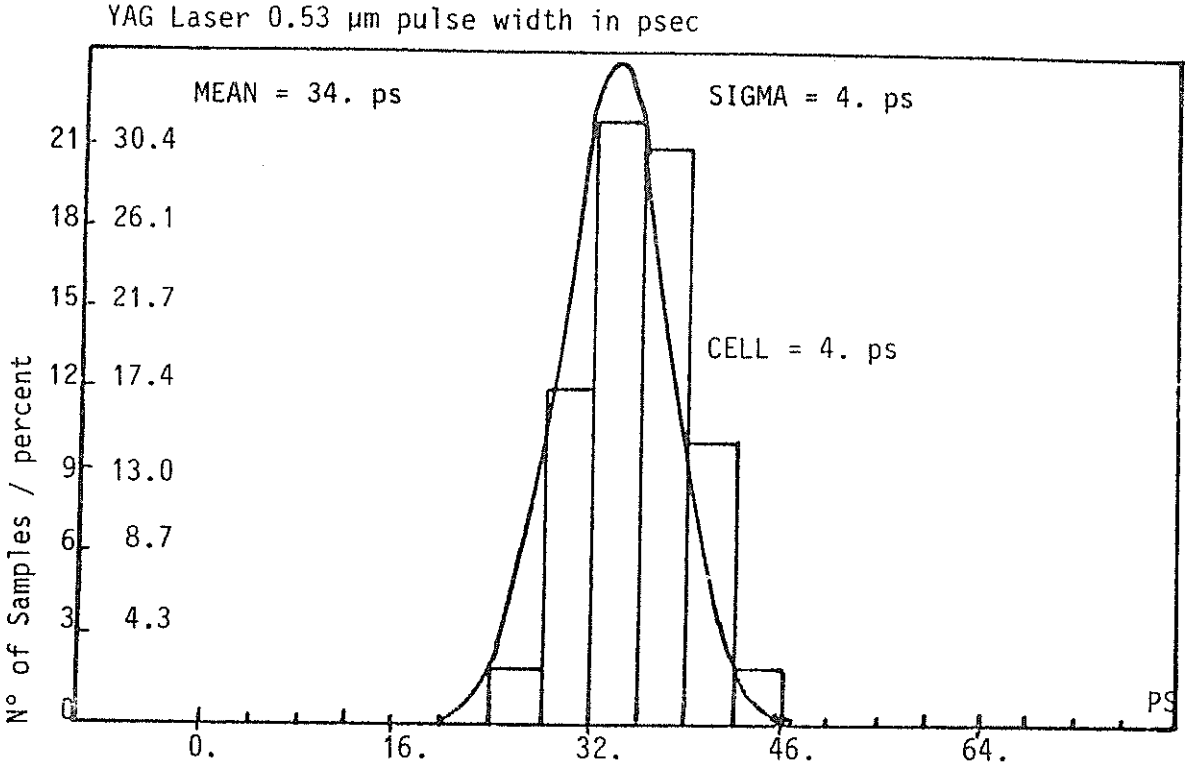

HISTOGRAM OF THE LASER 0.53 µm PULSE LENTH

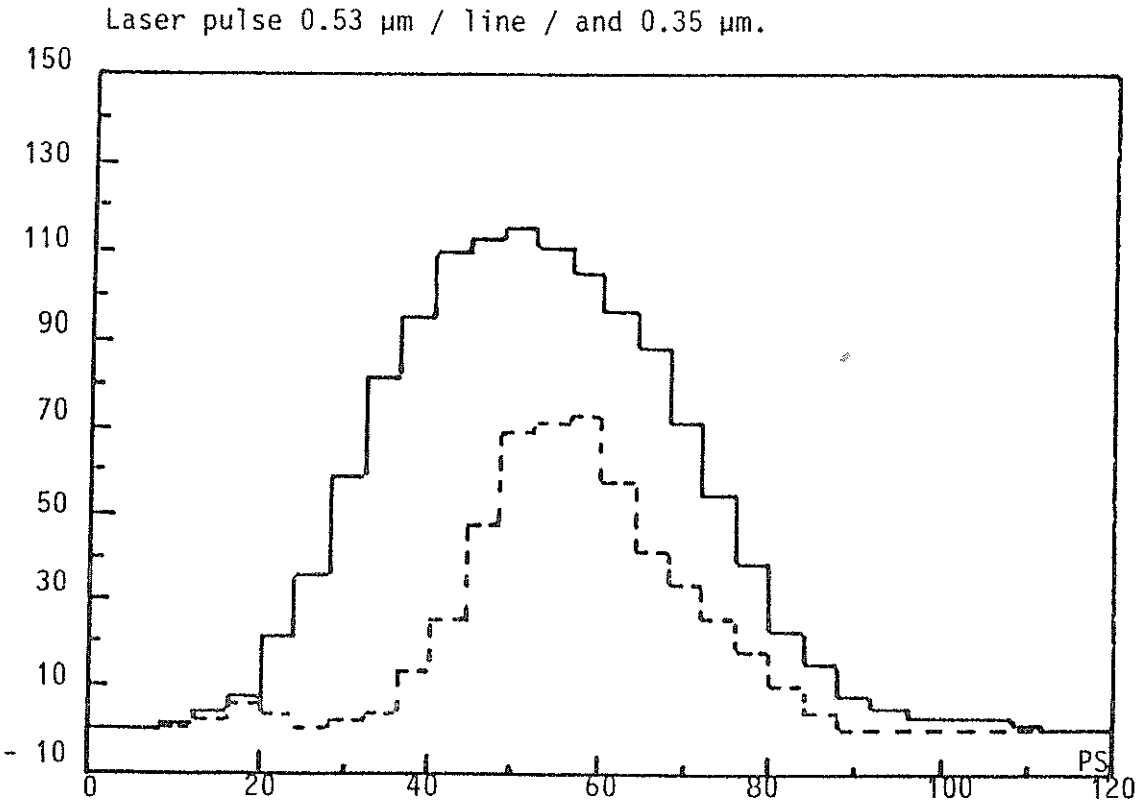

STREK RECORDS OF THE 0.53 AND 0.35 µm PULSES

Indoor 0.53/0.35 μm time delay / two windows /

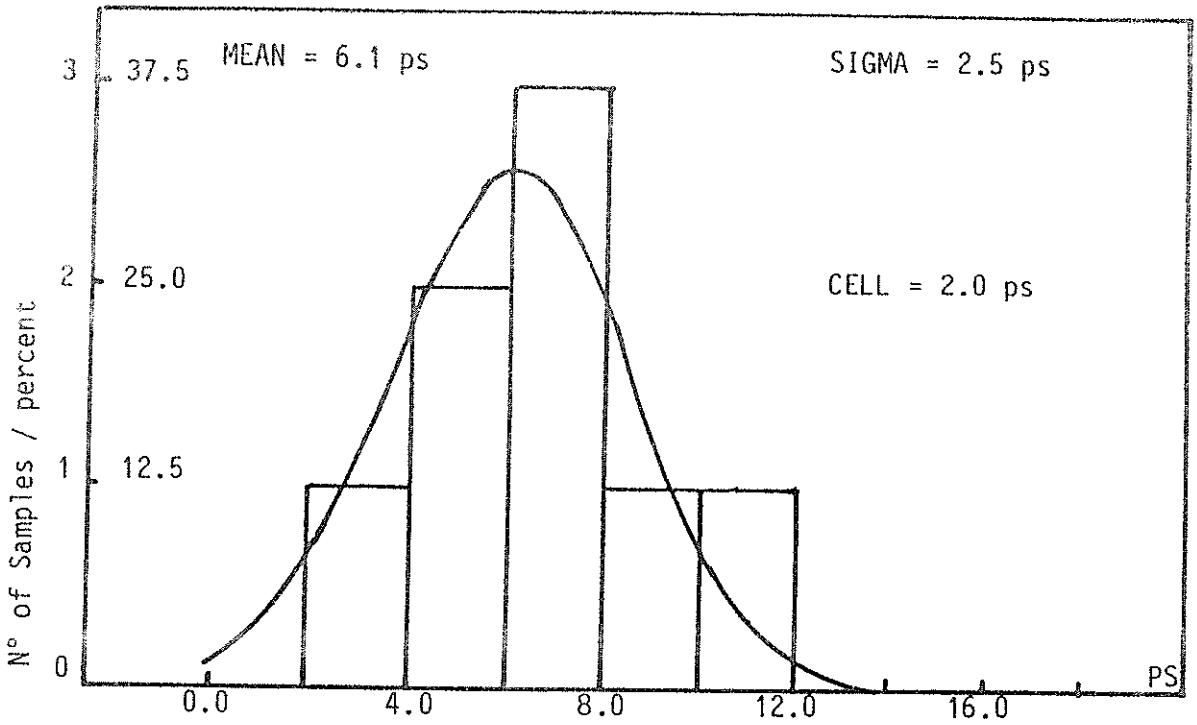

HISTOGRAM OF 0.53/0.35 μm TIME DELAY / INDOOR /

Green + Blue ext. target (106 m) ranging

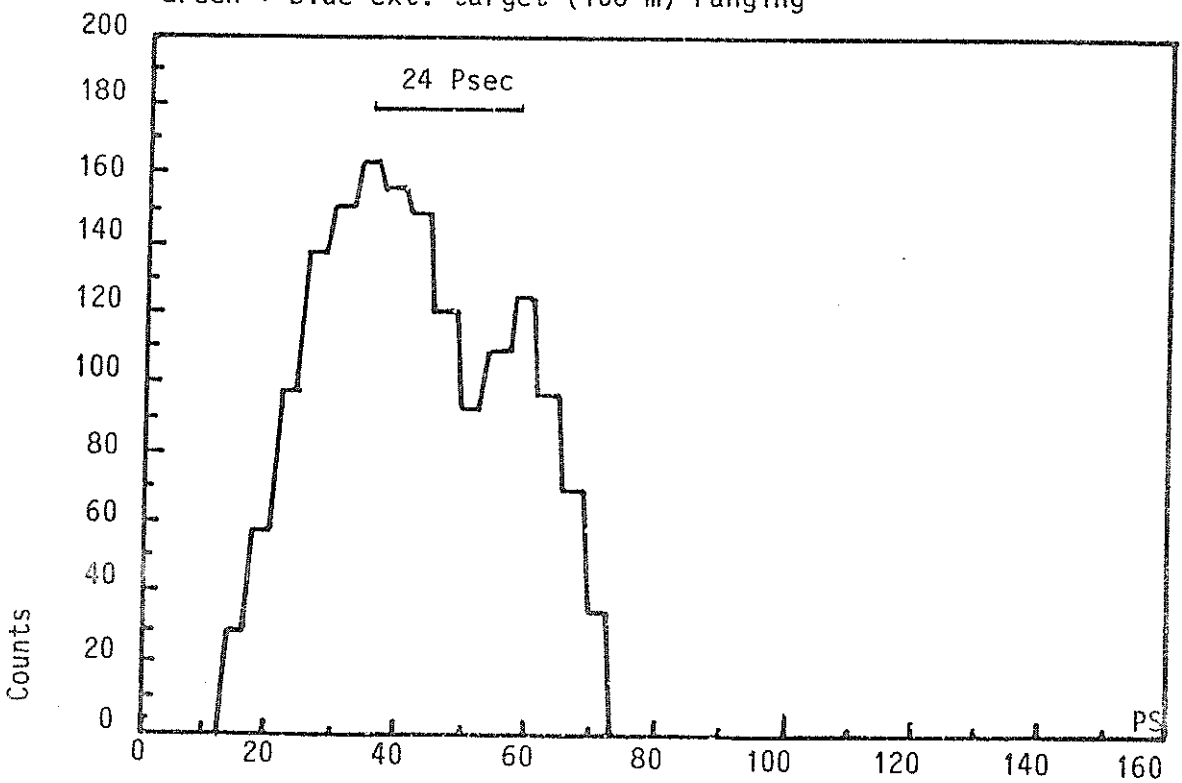

STREAK RECORD OF GROUND TARGET 0.53/0.35 μm RANGING

Ground target 0.53 /0.35 µm time delay (17.4.1984)

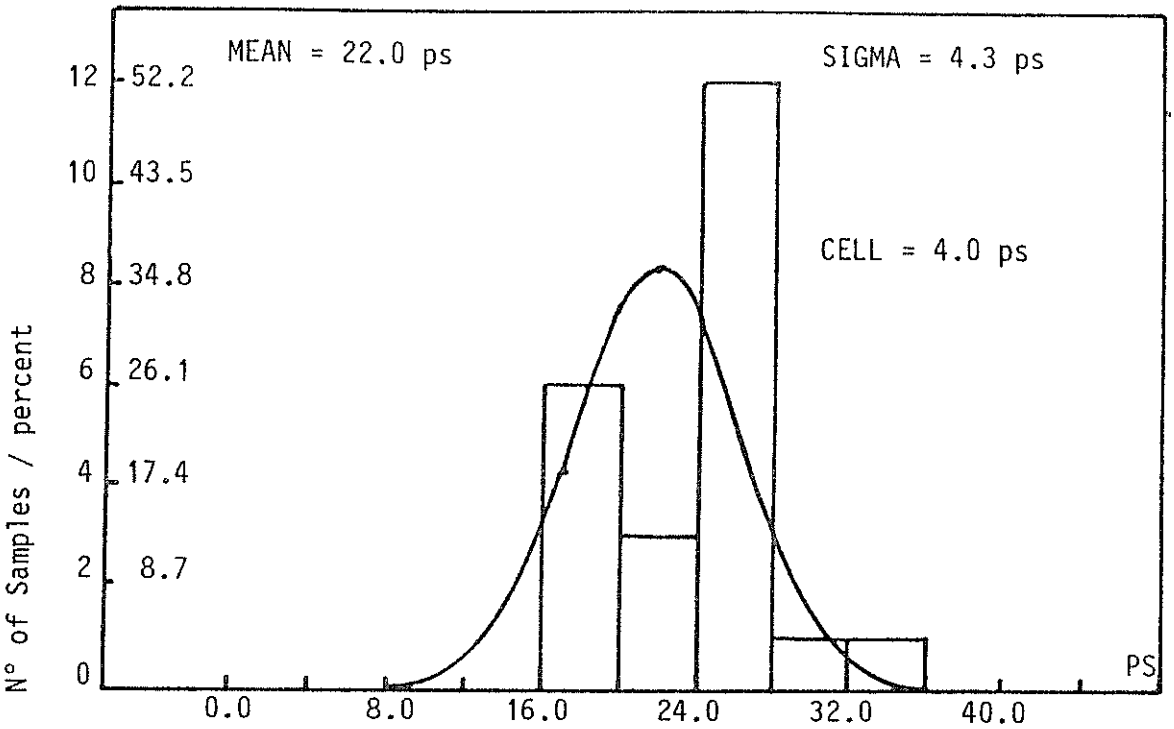

HISTOGRAM OF 0.53/0.35 µm DELAY / GROUND TARGET /

LASER RADAR INDOOR CALIBRATION EXPERIMENT

K. Hamal, I. Prochazka
INTERKOSMOS
Faculty of Nuclear Science and Physical Engineering
Czech Technical University
Brehova 7, 115 19 Prague 1 Czechoslovakia

Telephone (2) 84 8840
Telex 12 1254

J. Gaignebet
C.E.R.G.A.
Avenue Nicolas Copernic 06130 Grasse France

Telephone (93) 36 58 49
Telex 470 865

ABSTRACT

To range the satellites, we are using the train of picosecond pulses generated by Nd YAG oscillato/amplifier/second harmonic generator laser system. To establish an optimum discriminator/timing system, the indoor calibration experiment was carried out. The results indicate a limit single shot uncertainty 6cm RMS.

LASER RADAR INDOOR CALIBRATION EXPERIMENT

To obtain the system internal noise level below 10cm at the Interkosmos laser radar in Helwan /1/, the picosecond laser was implemented. To establish the optimal detector/discriminator/timing configuration, to decrease the ranging chain jitter and to increase the system stability, the extensive set of calibration experiments was completed. The aim of the calibrations was to measure the timing jitters of the most critical parts of the ranging chain.

The scheme of the calibration set up is on fig.1. The passively mode locked YAG laser /2/ generating a train of pulses was used. The resonator round trip time was 1.6nsec, The idividual pulse width 70 psec. Most of the energy was contained in 2-3 pulses. The laser output was frequency doubled to 0.53um. As the high resolution timing system, the Tranzient Digitizer Tektronix 7912AD, together with the appropriate software package, is used. The bandwidth of the system is 500MHz, its resolution is 512x1024 (time x amplitude) ,the fastest sweep is 1upsec/channel. The Tranzient is interfaced via HP85 to the master computer HP21MX with a 50MByte disc storage. The image data are recorded on line on the disc file with the repiate 0.3 frames/second. Completing the measurement series (100-500 events), the measured data are processed off line. A powerfull software package for data processing was prepared. It enables: smoothing the recorded images, pulse processing for radar purposes, modelling of various types of discriminators, computing the pulse amplitude, risetime, energy, etc. The triggering jitter of the Tranzient together with the proper function of the software were tested by the series of tests, using uniform calibration pulses. The measured trigger jitter was 25psec.

The START detector jitter calibration

To proceed the mode locked train of pulses properly, the special type photodiode/discriminator scheme is used /4/. The Tranzient is externaly triggered by the output signal of the START detector under test. The laser output signal, monitored by the fast photodiode, is displayed (the switch in a/ position). The time spread of the recorded pulses determines the detector jitter, its mesured RMS is 150psec. Simultaneously, processing the set of laser output records, the useful

information about the laser output stability, train length, etc. may be obtained /3/. The measured value of the START detector jitter is in table 1.

Single photoelectron PMT jitter calibration

The block scheme is on fig.1, the switch in position b/. The Tranzient was externaly triggered by the START discriminator pulse, the laser output pulse was attenuated and reflected to the PMT (RCA8852) input. The light was focused to the small area near the photocathode center. The PMT output signal was amplified by the 26dB/1200MHz amplifier and fed to the Tranzient. Using the ND filters, the received signal intensity was adjusted to single PE level (typically 100 echo PE from 1000-3000 laser shots). The no detected PE images were omitted, the recorded ones were processed by a program, which converts the data into the range values. Processing one image, four different range values are available, each one corresponding to one ideal discriminator of the type:

1. fixed threshold
2. constant fraction
3. centroid
4. maximum.

These range values were processed by the mode locked train YAG laser ranging data processing software package /5/. The resulting values of signle PE photomultiplier jitter are summarised in table 1. The lowest jitter was measured for an ideal constant fraction discriminator type (340psec).

PMT/discriminator jitter measurement

To determine the optimal PMT/discriminator (RCA8852/Ortec473A) configuration, the special experiment was carried out. Using the Tranzient digitizer the mutual position of the PMT output pulse and the discriminator output was measured. The PMT output pulse was devided, one part was fed to the discriminator input, the other was delayed and fed to the Tranzient input. The Tranzient was triggered by the discriminator output. The PMT dark noise signal was used for this test. The measured data were converted into the rangig data form using the software described above (constant fraction discriminator). Then, the jitter could be evaluated. This way, the deviation of the real constant fraction discriminator from the ideal one was determined.

Conclusion

The error budget of the laser radar ranging electronics was measured to be 0.41nsec (6cm). The main contribution to this value is due to the PMT RCA8852 single PE transit time jitter. To compare the indoor/outdoor measurements, the histogram of laser calibration series measured at the laser station in Helwan (July 1984) is shown on Fig.2. (In fact, the RCA31034A PMT is used on this station, but according to /7/,/8/ and our experience, their timing performance is the same.)

Literature

1/ K.Hamal,H.Jelinkova,A.Novotny,I.Prochazka,M.Fahim B.Baghos,A.G.Massevich,S.K.Tatevian, Interkosmos Laser Radar, Version Mode Locked Train, in this Proceedings
2/ K.Hamal, I.Prochazka,M.Cech,P.Hirsl,H.Jelinkova,A.Novotny, 2.Generation Laser Radar /INSATLAS2.2./ Mode Locked Train Experiment No.1 /indoor/, FJFI Preprint Series 191/83
3/ K.Hamal,I.Prochazka,M.Cech,P.Hirsl,H.Jelinkova,A.Novotny 2.Generation Laser Radar /Insatlas 2.2./ Mode Locked Train Experiment No. 2, FJFI Preprint Series No. 195/83
4/ M.Cech, Start Discriminator for the Mode Locked Train Laser Radar, in this Proceedings
5/ I.Prochazka, Mode Locked Train Laser Ranging Data Processing in this Proceedings
6/ EG&G Ortec 473a Constant Fraction Discriminator,Operating and Service Manual,USA
7/ R.W.Engstrom, RCA Photomultiplier Handbook published by RCA Solid State Division,Lancaster,USA,1980
8/ S.K.Poultney, Single Photon Detection and Timing: experiments and Techniques, Advaces in Electronics and Electron Physics, Vol.31, Academic Press, New York 1972

START detector		150 psec	/4/
PMT (RCA8652)	fixed threshold	(350 psec)	
	constant fraction	340 psec	applied
	centroid	(350 psec)	
	maximum	(470 psec)	
STOP dicriminator (Ortec 473A)		100 psec	/6/
flying time counter (HP5360)		150 psec	
Ranging electronics error budget		410 psec (6cm)	
		**********	

Table 1.

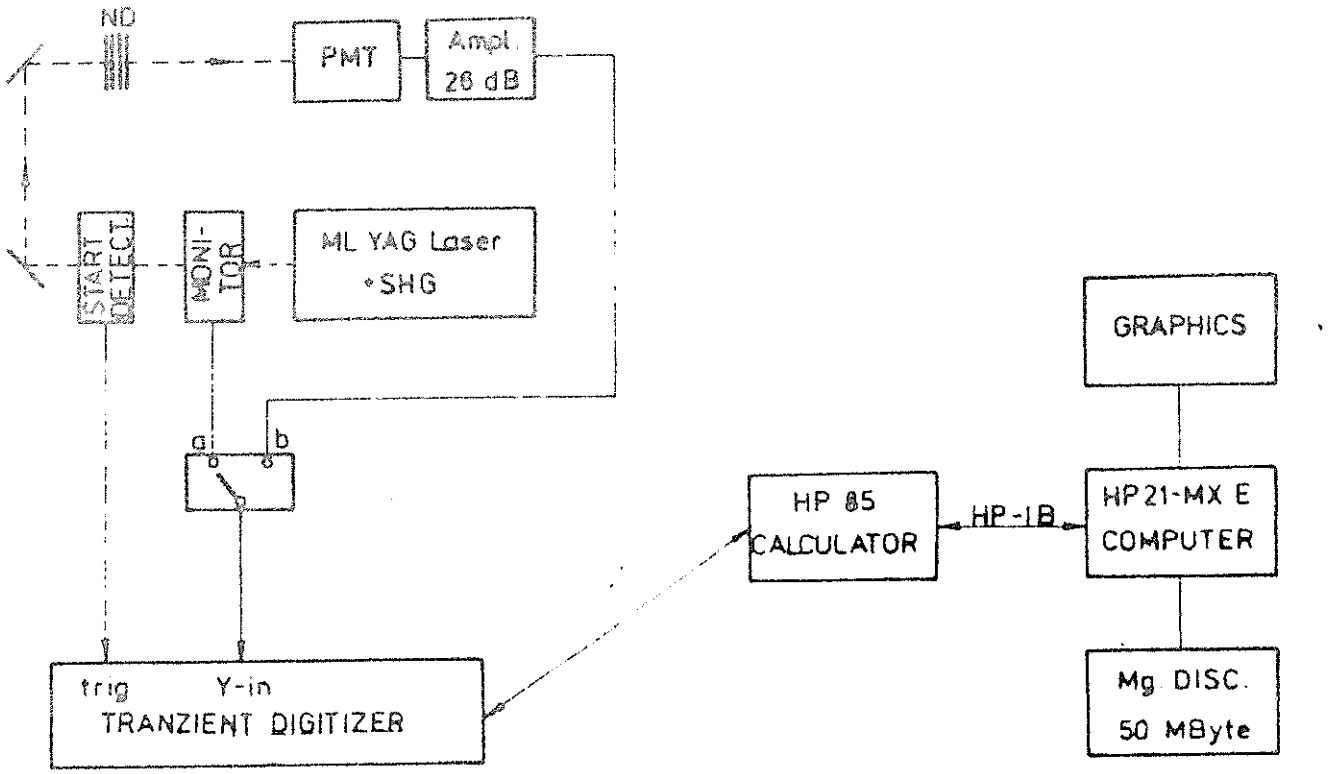

Indoor calibration experiment block scheme.

Fig. 1.

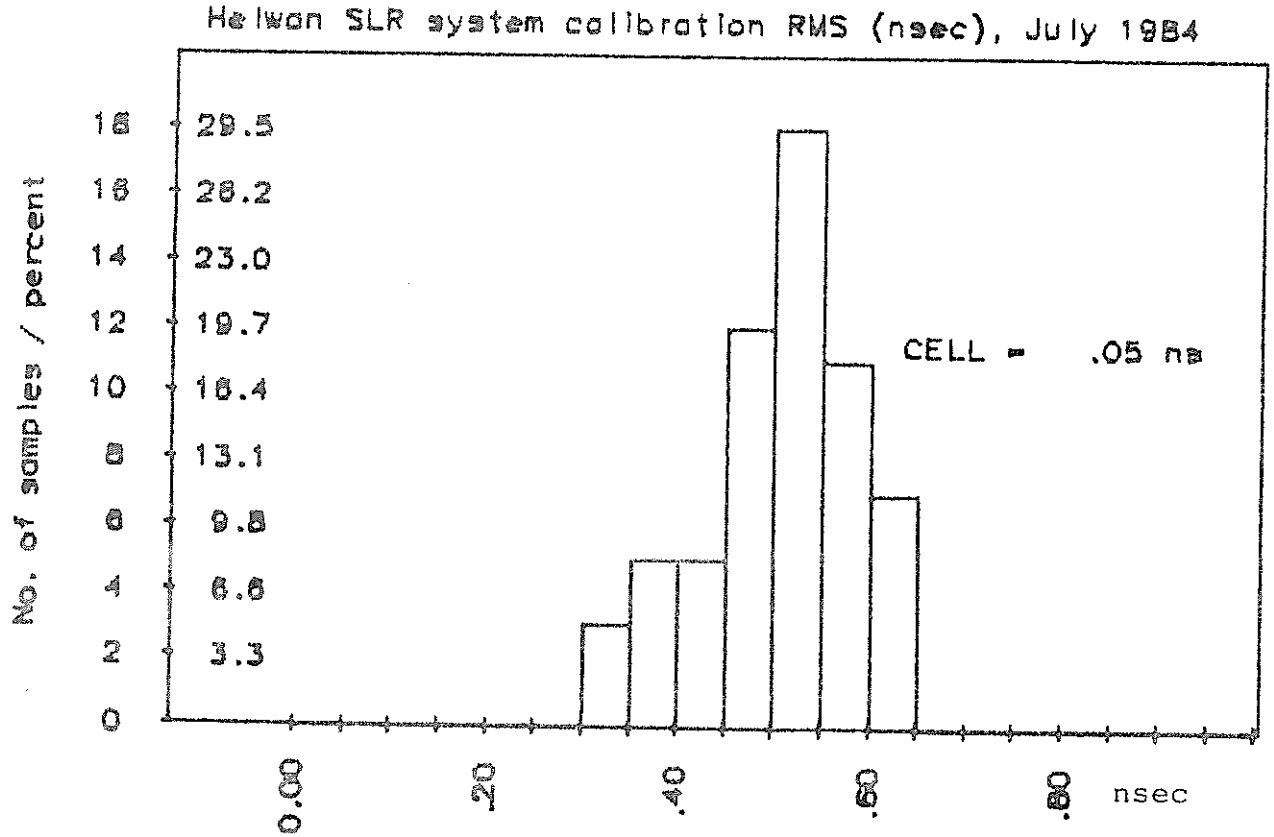

Histogram of SLR system calibration /internal pass/ RMS, station Helwan, period July 1984.

Fig. 2.

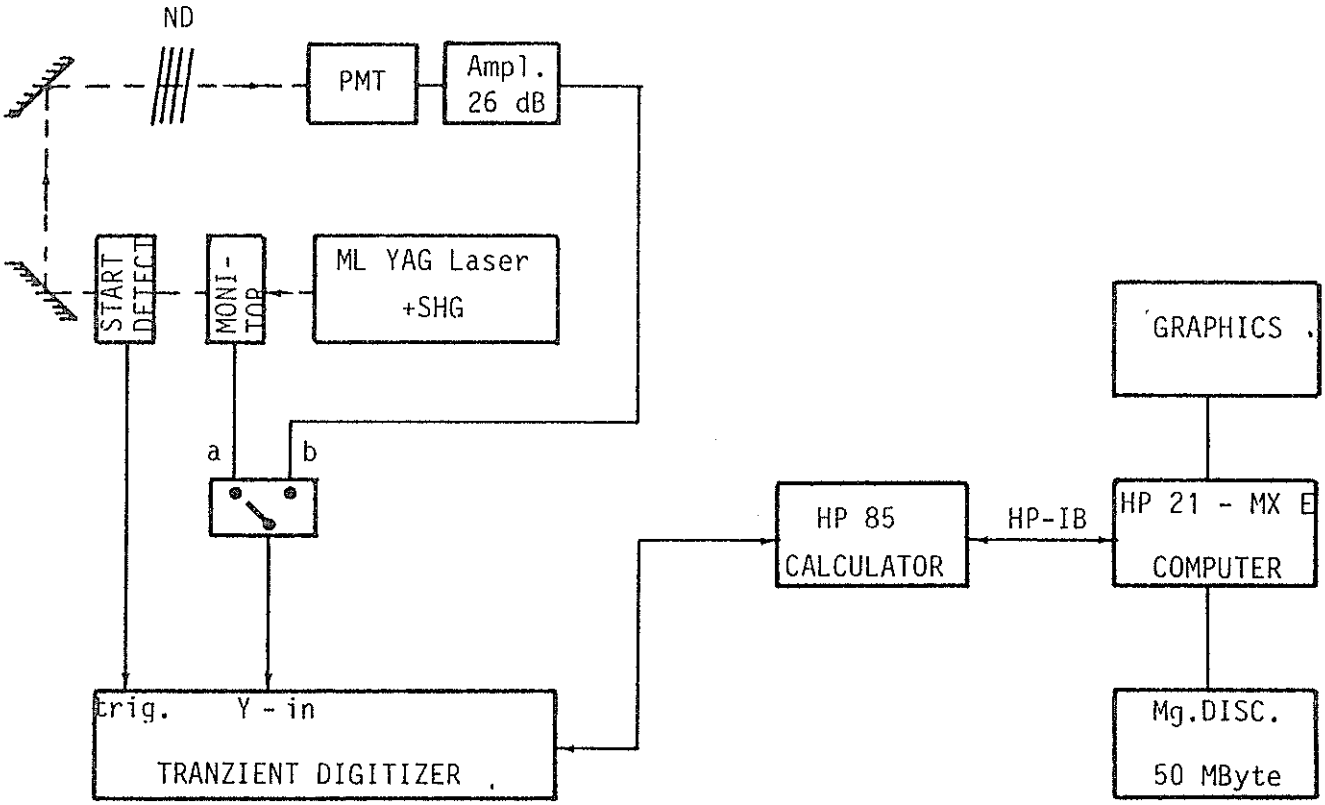

INDOOR CALIBRATION EXPERIMENT BLOCK SCHEME

- FIG. I -

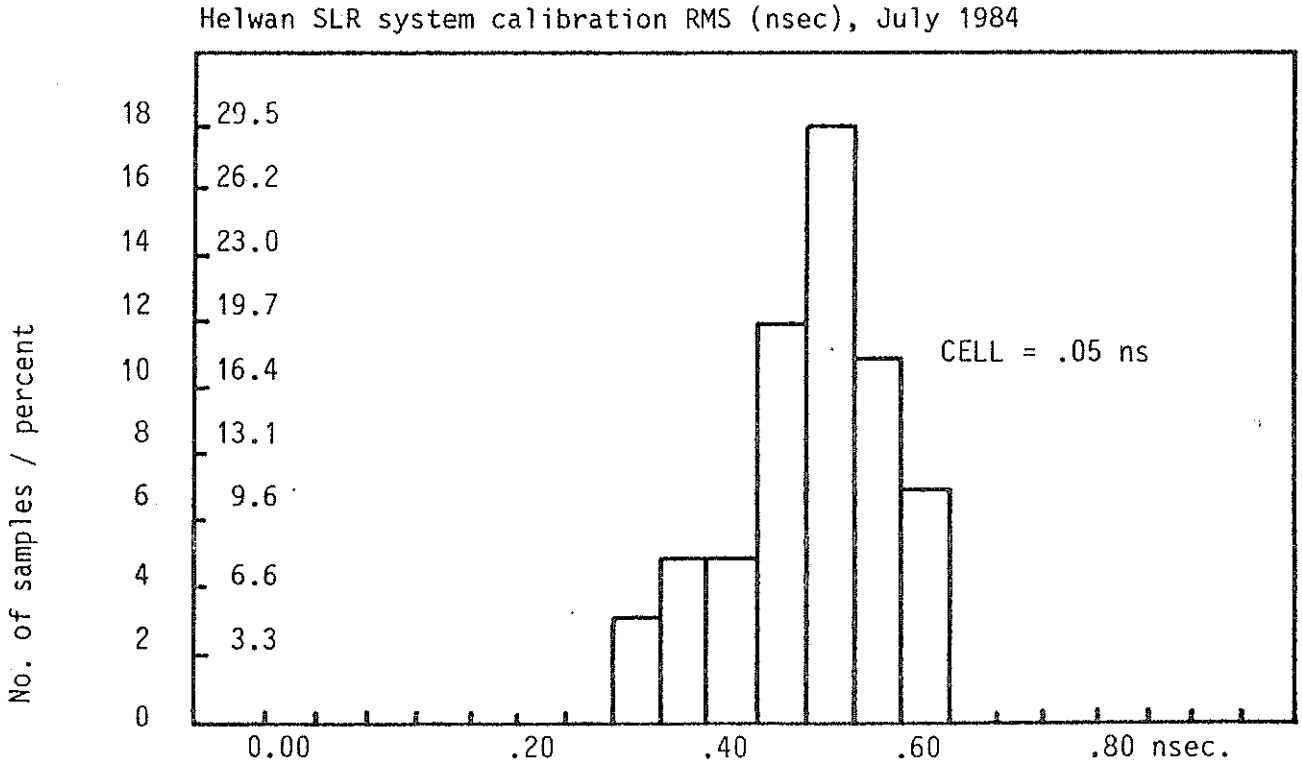

HISTOGRAM OF SLR SYSTEM CALIBRATION /INTERNAL PASS/ RMS, STATION HELWAN, PERIOD JULY 1984.

- FIG. II -

FURTHER DEVELOPMENT OF THE NLRS AT ORRORAL

B.A. Greene
Division of National Mapping
PO Box 31
Belconnen ACT 2616 Australia

Telephone 062 525095
Telex 62230

ABSTRACT

The recently commissioned Natmap Laser Ranging System is described and some initial performance figures given. The development program for the system is briefly outlined. The fundamental goals of the program are to maximise precision, accuracy, and efficiency in SLR and LLR modes. From an initial capability near the state of the art, developments are outlined which will produce sub-centimetre SLE precision to any satellite within 10 seconds under even marginal meteorological conditions over the next 12 months. Preliminary considerations of multi-Gigawatt LLR lasers and multi-wavelength SLR are given.

FURTHER DEVELOPMENT OF THE NLRS AT ORRORAL

1. Current Status

The Natmap Laser Ranging System (NLRS) is now fully operational to LAGEOS, and is under development for Lunar ranging operations in late 1984. The principal characteristics of the NLRS can be given as:

Telescope aperture	:	1.5 metre
Pointing accuracy	:	3 arc seconds
Laser	:	QUANTEL YG402-AP
Computer System	:	HP A700
Receiver	:	RCA 31034A
Single shot precision	:	7 cm
10 second precision	:	1 cm (LAGEOS)

The NLRS is currently performing adequately to LAGEOS, obtaining 5-15000 hits/pass, depending on conditions. It has a day/night capability.

2. Short Term Developments

The random current errors of the NLRS are due to:

Laser pulse width	:	300 ps
PMT/Receiver	:	400 ps
Timing	:	200 ps

These represent the NLRS at initial configuration, which will be altered for the first 4-5 months of operation.

Commencing early in 1985, several changes will be made to the system which will improve performance. The laser pulse width selected will be reduced to 50 ps for all SLR operations. The PMT will be replaced by a new Microchannel Plate PMT with a Transit-Time jitter specification of 100 ps (max), and a rise time of 30 ps (max).

These modifications alone should reduce the single shot uncertainty to better than 4 cm, and the 10 second normal point precision to 6 mm (for LAGEOS).

Other significant improvements planned for 1985 are in the AUTOTRACK capabilities of the system. Currently, a significant proportion of the LAGEOS data is obtained without any operator assistance in guiding (i.e. absolute pointing to LAGEOS). It is expected that as the station coordinates of the site become better defined and our in-house ability to 'improve' our predictions using previously observed data improves, the dependence upon an operator will diminish significantly. The goal is to obtain 100% of LAGEOS observations without operator intervention in the long term.

The AUTOTRACK developments extend also to LLR observations. Since the mount model for the 1.5m telescope can be better than 3 arc seconds on any night (it is not stable at this level for more than 1 night), absolute pointing and guiding seems feasible, perhaps with some minimal search pattern capability added.

3. Long Term Developments

3.1 SLR Precision

The single largest error in the ranging system after the laser and receiver have been modified (above) will be the timing system (200 ps/event). An improvement in this area to 50 ps would give 2 cm single-shot precision immediately. A multi-stop, 50 ps precision timing system is under development.

If the laser is tuned to 30 ps pulse width, the system error budget becomes:

Laser	:	30 ps
Timing	:	50 ps
PMT/Receiver	:	100 ps
RSS		116 ps or 1.8 cm

Theoretical studies are currently being undertaken into the viability of using a streak camera as an additional vernier for the timing system to give 10 ps precision. Preliminary work indicates that the total random error budget for such a system could be 50 ps, resulting in sub-centimetre single shot precision.

3.2 LLR Data Density

The single most effective way of improving LLR system performance is to increase the laser power. Such a development is being considered for Orroral. The objection is to obtain 300 mJ in a single 100 ps pulse, or 800 mJ in a train of four 100 ps pulses, at 10 Hz. Alternatives to slab laser configurations are being actively pursued, and some feasible designs have been put forward which would reach the performance goal without the need for a slab. However, very significant performance improvements for Nd:YAG lasers will come from solid state pumping systems now under

development in other laboratories. If adequate performance can be maintained in the short term using the existing laser, then it is likely that further development of the laser will await developments in solid-state pumping.

3.3 Multiple Wavelength Ranging

Even preliminary examination of the two wavelength technique reveals the considerable difficulties inherent in the technique. However, if SLR ranging will be, from 1985, of 1 cm precision (normal point) for a large proportion of the ranging stations in operation, then it may be necessary for one or two stations to acquire a data base of two colour ranging data for purposes of 'calibrating' the atmospheric correction formulae. The Orroral system has some unique advantages for performing this experiment.

1. large telescope with very precise pointing and high quality Coude optics

2. extensive computing facilities on site

3. extensive optical and electronic facilities

4. colocation with a national time and frequency calibration laboratory

5. site weather characteristics much like most of the rest of the network.

For these reasons the topic is kept under review, so that when the accuracy requirement for SLR exceeds 1 cm, a decision could be made to attempt to range at more than one wavelength.

The streak camera which can operate as a 10 ps timing vernier can be adapted to determine the differential return epoch of the two returns with 10 ps (possibly even better) precision.

AN OVERVIEW OF NASA AIRBORNE AND SPACEBORNE LASER RANGING DEVELOPMENT

J.J. Degnan
Instrument Electro-Optics Branch, code 723
NASA Goddard Space Flight Center
Greenbelt, MD 20771 USA

Telephone (301) 344 7000
TWX 710 828 9716

ABSTRACT

Beginning in the mid-Seventies, there was a great deal of scientific and technical interest in the development of a Spaceborne Geodynamics Ranging System (SGRS) which would be capable of making global geodesy measurements to a dense network of relatively inexpensive, passive, ground-based retroreflectors. It was argued that such a system would provide a vastly larger and more timely data set for the study of tectonic plate motion and regional crustal deformation relative to what could reasonably be achieved with ground-based satellite laser ranging (SLR) systems. The data could be further augmented and densified through the development and use of relatively low cost aircraft-based systems. Modest funding during the period from 1975 to 1983 permitted the completion of various fundamental engineering, scientific, and simulation studies and the development of several prototype hardware components and software packages. The present article gives a brief history of NASA and recent European efforts in airborne and spaceborne laser ranging, summarizes the scientific ans technological achievements, provides a bibliography which permits readers to obtain more detailed information, and speculates on possible future development activities.

AN OVERVIEW OF NASA AIRBORNE AND SPACEBORNE LASER RANGING DEVELOPMENT

Beginning in the mid-Seventies, there was a great deal of scientific and technical interest in the development of a Spaceborne Geodynamics Ranging System (SGRS) which would be capable of making global geodesy measurements to a dense network of relatively inexpensive, passive, ground-based retroreflectors. It was argued that such a system would provide a vastly larger and more timely data set for the study of tectonic plate motion and regional crustal deformation relative to what could reasonably be achieved with ground-based satellite laser ranging (SLR) systems. Furthermore, it would accomplish this feat at a greatly reduced cost. Modest funding during the period from 1975 to 1983 permitted the completion of various fundamental engineering, scientific, and simulation studies and the development of several prototype hardware components and software packages.

The original system concept assumed a Space Shuttle-Borne system which utilized a frequency-doubled, Q-switched Nd:YAG laser with a seven nanosecond pulsewidth as the source. This concept was driven, to a very large extent, by the availability of relatively compact, hardened military lasers which had flown and operated successfully in rather hostile, high altitude, fighter aircraft environments. A reasonably concise account of the spaceborne concept and simulations of system performance can be found in references 1 and 2. A detailed engineering analysis is available in reference 3 and a summary of the proposed science applications can be found in reference 4.

It soon became apparent, however, that the anticipated 10 to 20 cm accuracy of the system was not going to satisfy the rapidly burgeoning number of science applications which were now demanding accuracies on the order of one to two centimeters. This fact spurred NASA to develop space-qualifiable prototype components which would permit ranging from a space platform to ground-based retroreflectors with centimeter accuracy. These included: (1) a compact, 10 mJ (green), 200 picosecond pulse, modelocked Nd:YAG laser transmitter[5,6]; (2) a low time walk constant fraction discriminator[7]; (3) a 19.7 picosecond resolution event timer (ET)[8]; (4) a 9.7 picosecond resolution time interval unit[9,10]; (5) a high-speed, arcsecond accuracy pointing mount and all-digital controller[11,12]; and (6) large cross-section, ground reflectors. In addition, developmental work began on a circularly scanned streak tube (CSST) receiver intended to improve the receiver impulse response by almost two orders of magnitude[13]. The latter acts as a vernier on the "coarse" receiver which primarily consists of a high-speed photomultiplier (e.g., the ITT 4129 microchannel plate photomultiplier having a 450 picosecond impulse response), a low time walk discriminator, and a high-resolution time interval unit.

The transmitter/ "coarse" range receiver combination typically yields 5 millimeter one sigma precisions in horizontal range experiments over kilometer long paths. Bias errors in the range map to a fixed retro-reflector are at the subcentimeter level as reported previously[14]. The limiting resolution of the prototype CSST receiver (when the program was terminated due to funding cuts) was about 33 picoseconds and was due to an inability to focus the electron beam image adequately within the tube.

The SGRS pointing system requirements were rather unique in that, in addition to being able to track with arcsecond precision at rates up to two degrees per second, the system required a slew velocity of 200°/sec and a maximum angular acceleration of 500°/sec^2 in order to acquire and track multiple ground based targets. The final engineering prototype met all of the SGRS requirements. The tracking mount supports a 32cm by 19cm elliptical mirror constructed of lightweight beryllium. Sixteen-bit incremental optical encoders, augmented by precision measurements of the phase of the quadrature detector outputs, yield an effective 23-bit resolution angular position in each of the two axes. The optical mount is driven by a "smart" all-digital, microprocessor-based controller. This frees up the main driving computer by requiring tracking updates only once a second consisting of a position, angular velocity, and angular acceleration. The microprocessor interpolates between updates using the resulting second order polynomial in the time variable at a rate of 512 times per second for each axis. Math models for system dynamics, bearing friction, stiction, etc., are used in Kalman Filtering algorithms to maintain system pointing and tracking accuracies. A plot of the measured RMS tracking jitter versus tracking rate is shown in Figure 1. Except near the maximum tracking rates, the tracking jitter is at the subarcsecond level. A more complete written description of the full range of pointing system tests and results is in preparation.

In 1979, the original SGRS hardware was upgraded to a subnanosecond system based on the previously mentioned hardware prototypes and renamed the Global Geodynamics Ranging System (GGRS). The GGRS was reconfigured as a free flyer instrument compatible with the Multimission Modular Spacecraft (MMS)[15]. The latter spacecraft can be launched from either Shuttle or NASA's Delta Rocket. The proposed GGRS package included two modelocked transmitter heads with a single power supply in order to extend the mission life to approximately 3 years for a combined geo-dynamics and ice altimetry mission. The GGRS concept did not incorporate the CSST receiver since the latter was still undergoing development.

Unfortunately, the funding necessary to begin development of a fully space-qualified system never materialized. Thus, in 1980, a concept for a six beam Airborne Laser Ranging System (ALRS) was developed[16,17] as an intermediate, low-cost, alternative which would simultaneously provide useful geophysical data on a regional scale and demonstrate the technical feasibility of the global spaceborne system. In these earlier versions of the ALRS, we planned to use a LORAN C navigator and a pressure altimeter to provide navigational updates to the aircraft to aid in acquisition and tracking of the ground retroreflectors. In the most recent version, however, we propose to use a GPS receiver to update the three position

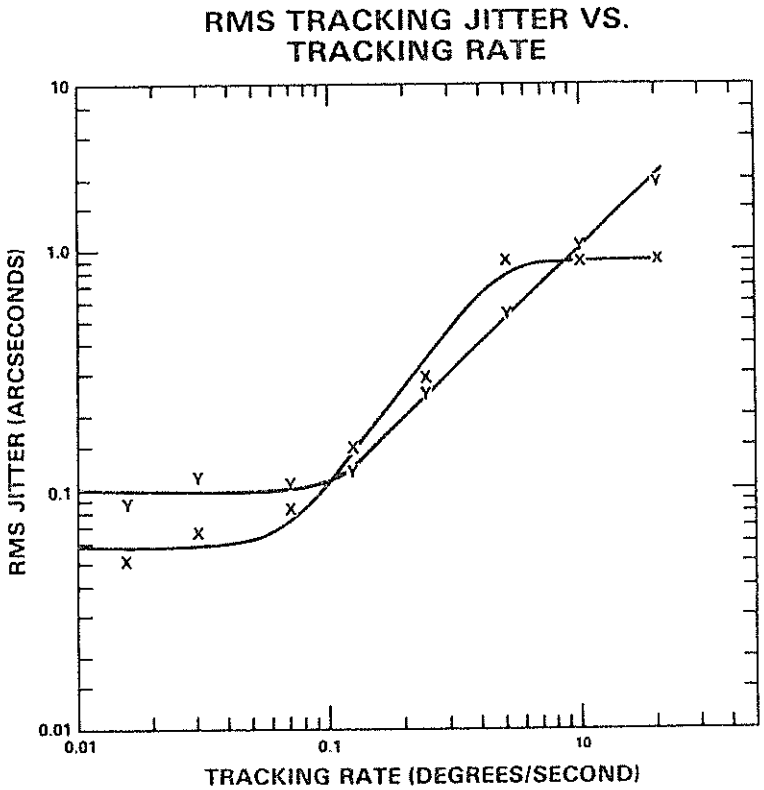

FIGURE 1: ROLL (X) AND PITCH (Y) TRACKING JITTER

coordinates since the GPS system is now nearing operational status. A block diagram of the current scheme is shown in Figure 2. From 1980 to 1982, the ALRS was actively studied and simulated. The NASA Lockheed Orion was chosen as the host aircraft. From this aircraft, baseline precisions of 1 cm per 30 Km of baseline could be achieved. High flying aircraft, such as NASA's ER-2 research aircraft, would yield the same precision over 100 Km baselines. Optomechanical designs for the ALRS were generated, components were procured, and assembly of selected subsystems was begun. The development of operational, navigational, and data analysis software packages was well underway. Target sites in the area of Shenandoah, Virginia, were chosen for the initial test flight. The Shenadoah area is convenient to the Goddard Space Flight Center and to the aircraft's home field at Goddard's Wallops Flight Station, has a terrain which varies widely in altitude above sea level thereby simulating most of the interesting fault regions, and contains approximately 17 first order survey monuments providing excellent ground truth information. Funding cuts brought all ALRS hardware work to a halt in 1982 but system simulations continued into 1983.

In an attempt to salvage the program, a concept for a greatly simplified (and even less expensive) airborne system was developed and named the Broadbeam Laser Surveyor (BLS)[18]. A block diagram of the system is shown in Figure 3. It uses a 100 mJ (green) modelocked laser such as the Quantel YG402 DP and distributes the energy over a 70 degree half-angle cone via an axicon. A matching, wide field-of-view receiver collects returns from any retroreflectors lying within the transmitter field-of-view and focuses them onto a single, high-speed photomultiplier. The system uses a multiple-stop time interval unit to record the multiple times-of-flight and contains no moving parts.

Operation of the BLS would be limited to low altitudes (less than 4 km) and to night flights due to the high daytime background noise resulting from the wide instrument field-of-view. The principal technology barrier to this instrument was the development of a practical receiver collecting lens which would simultaneously provide the ±70 degree field-of-view and an effective aperture on the order of two inches. Recent in-house studies have resulted in a realistic lens design. It is hoped that our basic advanced laser ranging funds will permit us to build and flight test a breadboard of this very simple system by 1986.

At the present time, NASA has no active program in the area of airborne or spaceborne laser ranging. However, during the past year, some discussions were held between the United States and Italy for a possible joint program to develop first the airborne and then a spaceborne system, but, to my knowledge, no agreement has yet been reached between the two countries. NASA/Goddard has recently proposed the single-color GGRS as an instrument on the Earth Observation System platform. The latter is a proposed experimental platform to be placed in an approximate polar orbit in the 1993 time frame and periodically visited and maintained, probably on a biannual basis, by crews from Space Station. The ability to refurbish the package on a periodic basis removes one of the major obstacles to the free flyer concept, i.e., the limited operating lifetime of the laser as

AIRBORNE LASER RANGING SYSTEM

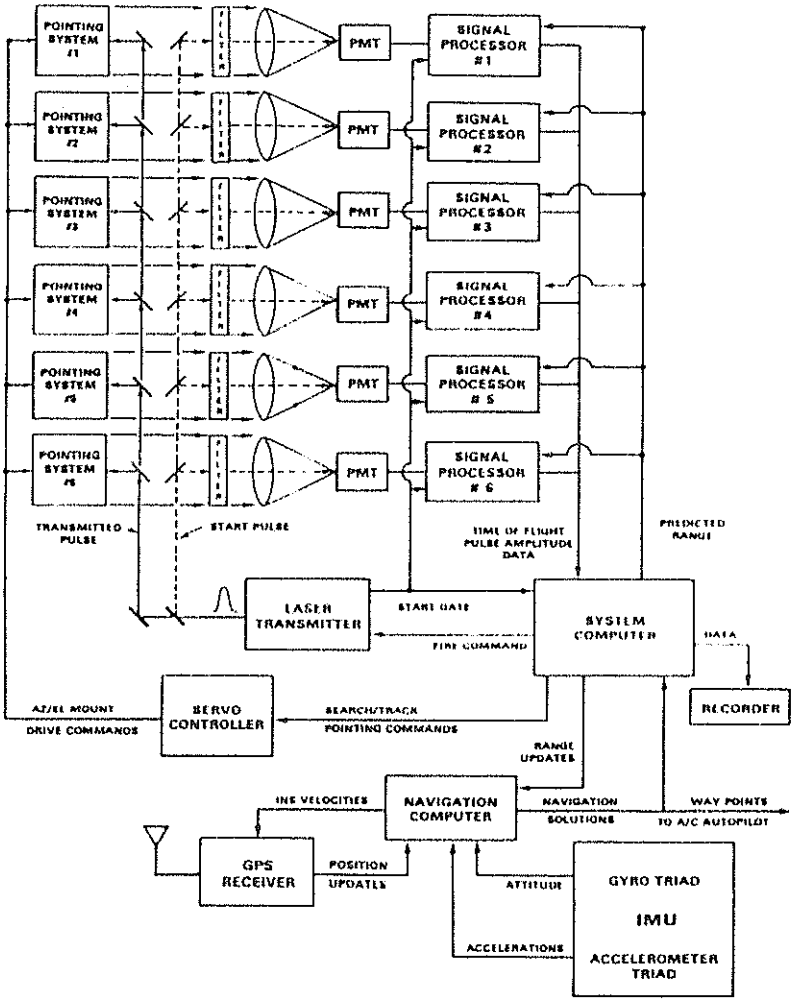

FIGURE 2

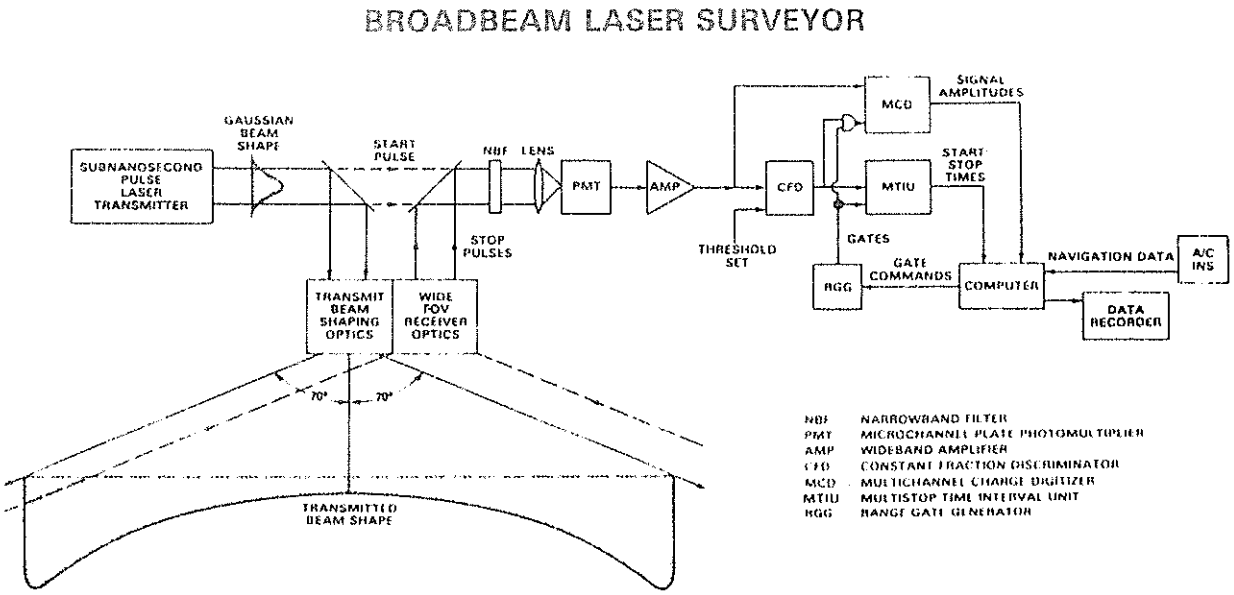
BROADBEAM LASER SURVEYOR
SUBNANOSECOND PULSE LASER TRANSMITTER
GAUSSIAN BEAM SHAPE
START PULSE
NBF
LENS
PMT
AMP
CFD
MCD
SIGNAL AMPLITUDES
MTIU
START STOP TIMES
THRESHOLD SET
GATES
RGG
GATE COMMANDS
COMPUTER
NAVIGATION DATA
A/C INS
DATA RECORDER
STOP PULSES
TRANSMIT BEAM SHAPING OPTICS
WIDE FOV RECEIVER OPTICS
70°
70°
TRANSMITTED BEAM SHAPE
NBF NARROWBAND FILTER
PMT MICROCHANNEL PLATE PHOTOMULTIPLIER
AMP WIDEBAND AMPLIFIER
CFD CONSTANT FRACTION DISCRIMINATOR
MCD MULTICHANNEL CHARGE DIGITIZER
MTIU MULTISTOP TIME INTERVAL UNIT
RGG RANGE GATE GENERATOR

FIGURE 3

determined by the flashlamp life (typically 10^7 shots). Alternate laser pumping schemes, however, such as pumping the Nd:YAG laser material with arrays of AlGaAs diode lasers may ultimately lead to a system with an operational lifetime two orders of magnitude longer.

Recently, a European group has studied a spaceborne laser ranging system which utilizes a two-color, picosecond pulse Alexandrite laser[19,20] and a second system which uses a CO_2 laser and superheterodyne transceiver[21]. NASA/Goddard also plans to explore mode- locked Alexandrite beginning in 1985. We have believed for some time that the fundamental and second harmonic frequencies of Alexandrite at 760 and 380 nm are near ideal for the two-color application because of their good atmospheric transmission, excellent detector quantum efficiencies, and good relative dispersion by the atmosphere. The wide gain bandwidth also permits the generation of pulsewidths on the order of a few picoseconds. One also eliminates the need for the relatively inefficient nonlinear generation of the third harmonic of Nd:YAG. The Alexandrite laser medium has a higher pump threshold than Nd:YAG, however, and therefore would require significantly more spacecraft prime power.

Spaceborne laser ranging faces stiff competition from proponents of the Global Positioning System (GPS) geodetic receiver approach who believe that their systems are also capable of yielding one centimeter accuracies in spite of a difficult water vapor calibration problem. The Global Positioning System satellite constellation is already partially in place and will almost certainly be completed. It therefore becomes a relatively inexpensive proposition to build and test geodetic receivers which make use of a system whose existence is a foregone conclusion even though the eventual operational costs of a global geodetic program might be prohibitively high. Furthermore, the GPS receivers have the decided political advantage that they are technically similar to devices already fielded by various user agencies and hence are a more "familiar" technology to those users.

A recent study[22] carried out by ORI, Inc., under contract to NASA Headquarters, compared the relative costs of a ten-year, global, geodetic campaign using on the one hand, GPS receiver techniques and, on the other, a spaceborne laser ranging system launched and periodically refurbished by the Space Shuttle. The study concluded that, within the probable error bounds (which in the present author's opinion are quite high), the ten-year costs of the GPS and GGRS approaches are comparable. The study did not attempt to address the relative quality of the data from a scientific standpoint.

REFERENCES

1. M. W. Fitzmaurice, P. O. Minott, and W. D. Kahn, "Development and Testing of a Spaceborne Laser Ranging System Engineering Model," NASA TM X-723-75-307, NASA/Goddard Space Flight Center, Greenbelt, MD 20771, USA, November 1975.

2. F. O. Vonbun, W. D. Kahn, P. D. Argentiero, D. W. Koch, and K. J. Eng, "Spaceborne Earth Applications Ranging System," NASA TM X-71035, NASA/Goddard Space Flight Center, Greenbelt, MD 20771, USA, December 1975.

3. E. A. Paddon, "Synthesis and Analysis of Precise Spaceborne Laser Ranging Systems," Final Report, McDonnell Douglas Astronautics Company-East, St. Louis, MO 63166, USA, Volumes 1 and 2 (MDC E1729), August 1977.

4. "The Report from the Workshop on the Spaceborne Geodynamics Ranging System," Institute for Advanced Study in Orbital Mechanics, The University of Texas at Austin, Austin, Texas, USA, IASOM TR79-2, March 1979.

5. R. H. Williams, L. L. Harper, and J. J. Degnan, "Ultrashort Pulse Solid-State Laser Development," presented at Laser '78, Orlando, Florida, USA, December 1978.

6. "Nd"YAG Laser Development for Spaceborne Laser Ranging System," International Laser Systems, Inc., Orlando, FL 32804, USA, NASA/GSFC Contract NAS5-22916, Phase I Final Report (February 1979), Phase II Final Report (December 1981).

7. B. Leskovar, C. C. Lo, and G. Zizka, "Optical Timing Receiver for the NASA Spaceborne Ranging System Part I: Dual Peak-Sensing Timing Discriminator, Lawrence Berkeley Laboratories. LBL-7274, NASA/Goddard Space Flight Center Contract NDPR S-40220B, January 1978.

8. B. Leskovar and B. Turko, "Optical Timing Receiver for the NASA Laser Ranging System Part II: High Precision Event-Timing Digitizer," Lawrence Berkeley Laboratories, LBL-6133, Lawrence Berkeley Laboratories, Berkeley, CA 94720, USA, LBL-8129, August 1978.

9. B. Turko, "A Picosecond Resolution Time Digitizer for Laser Ranging," IEEE Trans. Nucl. Sci., MS-25, No. 1, pp. 75-80, February 1978.

10. T. Zagwodzki, "Testing and Evaluation of a State-of-the-Art Time Interval Unit," NASA/Goddard Space Flight Center, Greenbelt, MD 20771, USA, TP-1051, September 1977.

11. "Final Technical Report: SGRS Pointing System Study, Volumes I and II," TRW Defense and Space Systems Group, Redondo Beach, CA 90278, NASA/GSFC Contract NAS5-23454, November 1978.

12. R. J. Brown, "Digital Control for the SGRS Mirror," Navtrol Company, Dallas TX 75243, USA, NASA/GSFC Contract NASA5-26891, January 1983.

13. C. B. Johnson, S. Nevin, J. Bebris, and J. B. Abshire, "Circular Scan Streak Tube with Solid-State Readout," Applied Optics, Vol. 19, pp. 3491-3495, October 1980.

14. J. J. Degnan and T. W. Zagwodzki, "A Comparative Study of Several Transmitter Types for Precise Laser Ranging," Proceedings of the Fourth International Workshop on Laser Ranging Instrumentation, Austin, TX, USA, pp. 241-250, October 1981.

15. "Global Geodynamics Ranging System (GGRS) Feasibility Study," General Electric Company Space Division, Valley Forge, PA, USA, GE Document No. 79SDS4245, NASA/GSFC Contract NAS5-23412, Mod. 175, August 1979.

16. J. Degnan, "Airborne Laser Ranging System for Rapid Large Area Geodetic Surveys," Proceedings of the Fourth International Workshop on Laser Ranging Instrumentation, Vol. II, Austin, Texas, USA, pp. 447-454, October 1981.

17. J. Degnan, W. Kahn, and T. Englar, "Centimeter Precision Airborne Laser Ranging System," J. Surveying Engineering, Vol. 109, No. 2, pp. 99-115, August, 1983.

18. J. Degnan, "Airborne Laser Ranging System for Precise Geodetic Surveys and Land Control," Proceedings of the International Symposium on Land Information at the Local Level, Orano, Maine, USA, August 9-12, 1982.

19. H. Lutz, W. Krause, and G. Barthel, "High Precision Two-Color Spaceborne Laser Ranging System for Monitoring Geodynamic Processes," Space 2000, pp. 236-254, 1983.

20. "Assessment of Technology Requirements Associated with Spaceborne Laser Ranging: SPALT Task 1 Final Report," Deutsches Geodätisches Forschungsinstitut, Munich, Germany, ESA Contract 4405/80/NL/HP(SC), DGFI Project No. 1/80/SPALT, June 1981.

21. "Study of Spaceborne Laser Range and range Rate Finder," Messerschmitt-Bolkow-Blohm GMBH, Space Division, RX12, Ottobrunn, Munich, Germany, ESTEC Contract No. 3883/79/NL/HP(SC), MBB Contact No. R 3700/2773 R, March, 1980.

22. E. Eller, N. Roman, and A. Wellen, "Life Cycle Cost Comparison of Four Space Technologies for Crustal Motion Measurement," ORI, Inc., Silver Spring, MD 20910, USA, May 1984 (draft), to be published.

SINGLE-SHOT ACCURACY IMPROVEMENT USING RIGHT FILTRATION AND FRACTION VALUES IN MULTI-PHOTOELECTRON CASE

W. Kielek
Faculty of Electronics
Technical University of Warsaw
00 665 Nowowiejska street 15 19 Warsaw Poland

Telphone 48 22 21007653 / 48 22 253929
Telex 813307

ABSTRACT

The approximate analytical formulas for the errors due to discrete generation and gain of photoelectrons and due to delay jitter in photomultiplier tube for the fixed threshold and constant fraction of the current and charge are given. The error is dependent on the filtration and fraction value. Also some simulation and experimental results are given, of reasonable agreement with the theory. Existing stations can be somewhat improved in some cases, using proper filtration and fraction values following the results presented.

SINGLE - SHOT ACCURACY IMPROVEMENT USING RIGHT FILTRATION AND FRACTION VALUES IN MULTI-PHOTOELECTRON CASE

1. Introduction

The signal at the anode of real PMT with the delay jitter is the same as in the case of ideal PMT without jitter, whose photocathode is illuminated by the equivalent signal pulse of the same energy, whose shape is the convolution of the signal pulse shape and the delay density curve of the real PMT. In the case of very short signal pulse, this equivalent shape is the shape of the PMT delay density curve only. Single - shot accuracy is dependent on the width of this equivalent shape. For the realisations of the received signal of more than single photoelectron, there exists the possibility to improve this accuracy using some processing of the signal, for example linear filtering before applying a constant or proportional threshold for the PMT current or charge. The part of the linear filter is the PMT itself, whose single photoelectron response curve convoluted with the pulse response of the eventual electric filter after PMT gives the response of the overall linear filtering. Author obtained the approximate analytical solutions for the error dependence on the filtration and threshold value, confirmed by simulation and experiment.

2. Results

Using some results of the inhomogeneous filtered Poisson process theory, one can obtain the formula for the normalised random time interval error, valid for all pulse signal shapes and all pulse responses of the filter in the limit case of sufficiently high number of photoelectrons in the signal:

$$\sigma_\Delta / T = g \alpha^{1/2} N^{-1/2} \qquad (1)$$

where: T is the measure of the equivalent signal pulse width, equal of the σ parameter of the gaussian equivalent signal pulse, or equal to the half of the width of equivalent signal pulse for the other shapes; α is the mean square of the normalised to 1 gain of the PMT tube; N is the mean photoelectron number in the signal; g - coefficient dependent on the shape of the equivalent signal, overall filter response shape and width, and on the threshold (fraction) value.

For the gaussian equivalent signal and filter response, g coefficient values vs fraction and filtration values are given by formulas (2), (3) and (4), and at the Fig. 1, 2, and 6, for the fixed threshold of the current, constant fraction of the current and constant fraction of the charge, respectively. Filtration parameter F at the Figs 1 and 2 is the filter res-

ponse width divided by σ parameter of the equivalent signal, when the z parameter in formulas is the square of the relation of σ parameter of the signal to σ parameter of the filter. Fraction f in the case of c.f. it is the fraction of the peak value in each realisation, when in the case of fixed threshold, it is the threshold value divided by the expectation of the peak value.

$$g^2 = \frac{(1+z)^2}{z \cdot \sqrt{2z+1}\; 2 f^2 \ln \frac{1}{f}} \cdot \exp\left(-2\,\frac{z+1}{2z+1}\ln\frac{1}{f}\right) \quad \ldots(2)$$

$$g^2 = \frac{(1+z)^2}{z \cdot \sqrt{2z+1} \cdot f^2 \ln \frac{1}{f}} \cdot \qquad (3)$$

$$\cdot\left\{\frac{1}{2}\exp\left[-2\,\frac{z+1}{2z+1}\ln\frac{1}{f}\right] - f\cdot\exp\left[-\left(\frac{z^2}{2z+1}+1\right)\ln\frac{1}{f}\right] + \frac{f^2}{2}\right\}$$

$$g = \left[2\pi f(1-f)\right]^{1/2}\left\{\exp\left[-(\text{inv erf}_* f)^2/2\right]\right\}^{-1} \qquad (4)$$

where $\text{erf}_* x = (1/\sqrt{2\pi})\int_{-\infty}^{x}\exp(-y^2/2)\,dy$

3. Comments

The results for the fixed threshold case are comparably poor (Fig 1); the best value of g is about 1.5. For the c.f. of charge, the results obtained for no additional filtration before integration of the current [formula (4)] are given at Fig. 6. The optimum fraction is 0.5, which holds also for any symmetric bell-shaped, triangular and other with distinct peak, shape of the equivalent signal. Using some linear filtration before the integration one can obtain g smaller than 1 (simulation results of Ojanen [1] and Kiełek). Bias changes with energy exist for the unsymmetric in time filter response only but are small (Fig. 5, simulations). For the fraction 0.5, this method is sometimes called as median, or half-area detection. The results for c.f. of the current are mostly surprising. The g coefficient improves and approaches 1, the value for some optimum estimation methods as conditional mean [2] and max. likelihood [3], when the filtration value F increases (Fig. 2). The optimum fraction value changes from 0.26 for small F values to 1 for $F > 2$ (Fig. 3). The dependency of g vs fraction f is small when F exceeds 4 (Fig. 2). The g coeff. is also energy dependent (Fig. 4, simulations), but for $F > 2$ the dependency is small for $N \geqslant 10$. Mean value of the result change vs energy are smaller when increasing F and f (Fig 7, simulations, filter response $\exp[-t/(5\tau)] - \exp(-t/\tau)$, and experiment).

4. Importance of the results obtained for the laser ranging

In the analogue signal processing case, use of the very high filtration F can be risky due to the threshold instability and electric noise. The F value of 4 ÷ 7 is recommended by author for the constant fraction of the current case, and also for the approximate max. likelihood implementation using the detection of position of the maximum of filtered signal [4]. This last case is also included in author's results (Fig 2), as the case of f ≅ 1. In the range of the width of laser pulse 2 ÷ 20 ns, this F value leads to the necessity to include some electrical filter after the PMT tube. Internal F value of PMT tube itself is 6 ÷ 12 for the RCA 8852, and 1.5 for new microchannel plate units. To set F at the proper value one can use approximate formula for the response width w_f of the additional electrical filter, at least 2-pole:

$$w_f = \left[\frac{F^2}{8\ln 2} \left(w_s^2 + w_j^2 \right) - w_p^2 \right]^{1/2} \quad \ldots\ldots\ldots \quad (5)$$

where w_s, w_p, w_j are the widths of: laser pulse, single photoelectron response of PMT, and PMT jitter density full width at half max , respectively. The need of additional filter exists when the right-hand side of (5) squared gives the value greater than zero. The need of the additional filter is strongest for the stations using wide laser pulses, but when using new microchannel plate PMT's, this need exists for all pulse widths used, also the smallest. The additional filter is not necessary in case of using the amplifier or other circuitry with the 3 db cut-off frequency $0.312/w_f$ or smaller.
The fraction value should be set as high as possible. The value f = 1 can be set using the differentiation, 35-40 db amplification, and zero-crossing detection.
Peak detection types of c.f. discriminators are preferable, but there is the lack of this type instruments at the market. In case of using c.f. discriminator used in scintillation-counter technique, for instance ORTEC 473 or similar, there is the need to lengthen the delay line to the value of delay

$$t_d = \frac{1}{2} \sqrt{\frac{w_p^2 + w_f^2}{\ln 2} \ln \frac{1}{f}} \quad \ldots\ldots\ldots \quad (6)$$

5. Conclusion

Existing stations having multi - photoelectron returns and using MCP type of PMT's, or in case of other PMT's, using pulse widths greater than 2 ns, can be somewhat improved by using enough analog filtration (Fig. 2).
Above holds for the stations using c.f. discriminators and approximate max. likelihood estimation as well. For the fixed threshold, use of Fig. 1 can decrease the error.

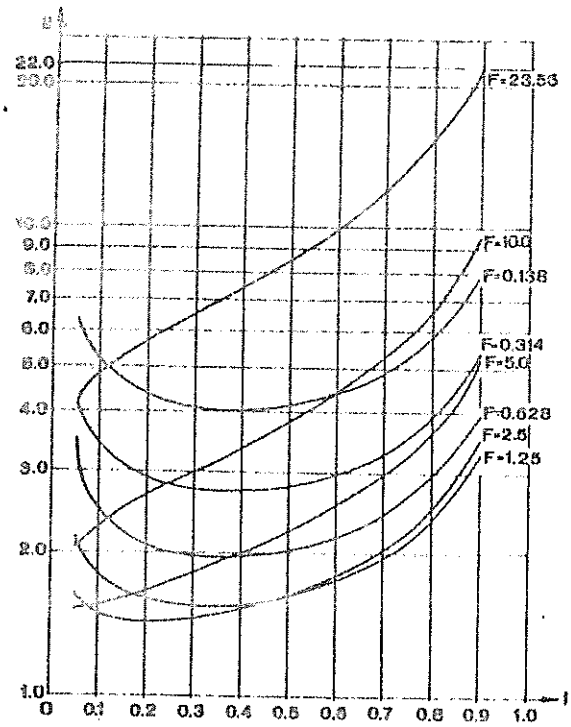

Fig.1. g coeff./form.2/

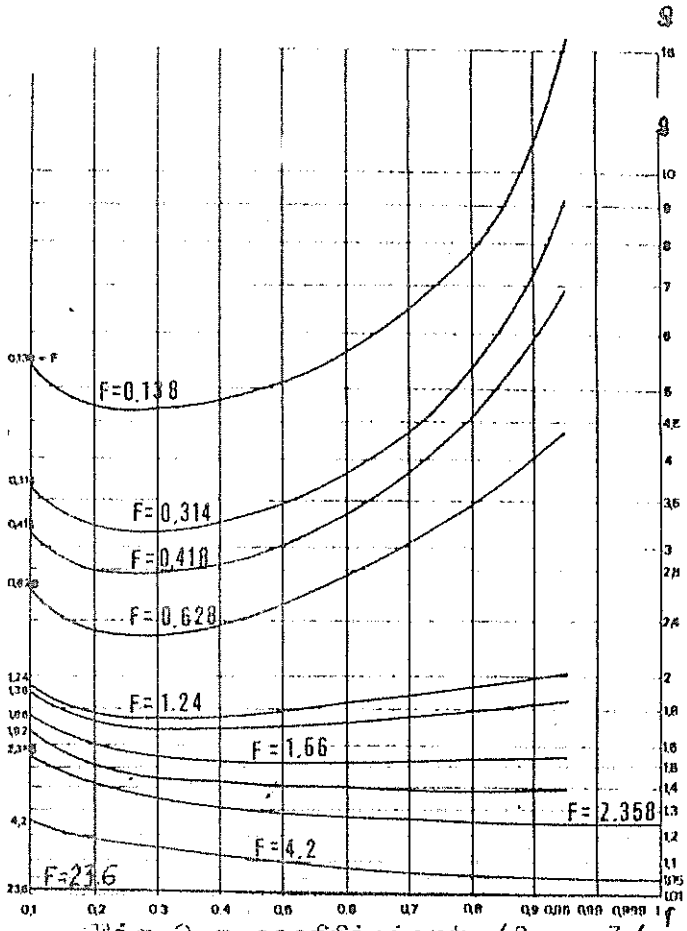

Fig.2. g coefficient /form.3/

Fig.4. g coeff.vs energy

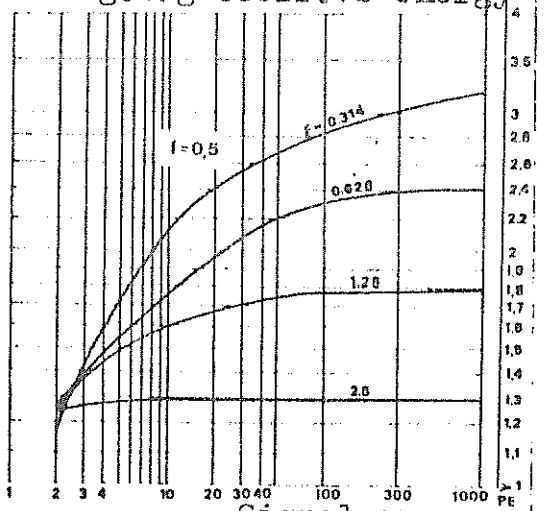

Signal energy

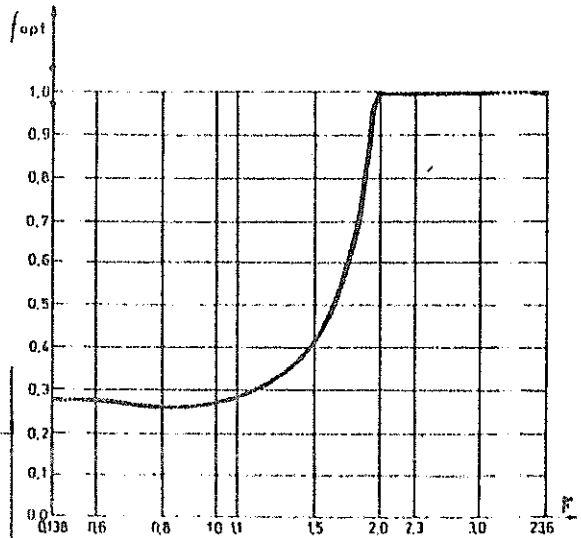

Fig.3 Optimum fraction $f_{opt.}$ vs.filtration F for c.f. of current

FIG.6

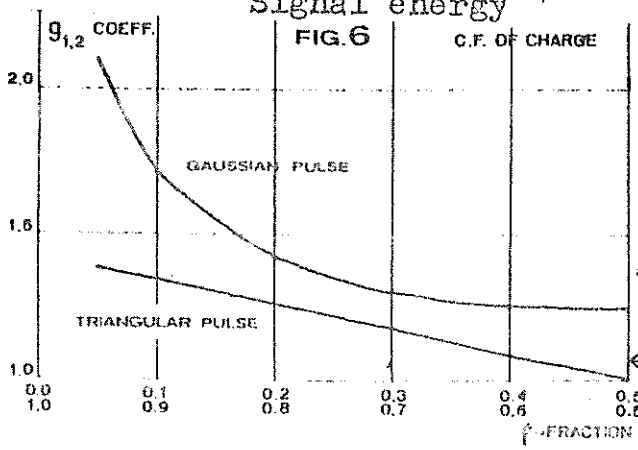

←Fig.6. g coeff./form.4/

REFERENCES

1. O.Ojanen, Reports of the Finnish Geodetic Institute No.79: 1,1979
2. I.Bar-David, IEEE Transactions on IT, May, 1975, pp.326-330.
3. I.Bar-David, IEEE Transactions on IT, vol.IT-15, No1, Jan. 1969, pp.31-37.
4. J.B. Abshire. IV-th Laser Workshop Proceedings, Vol.II. p.339.

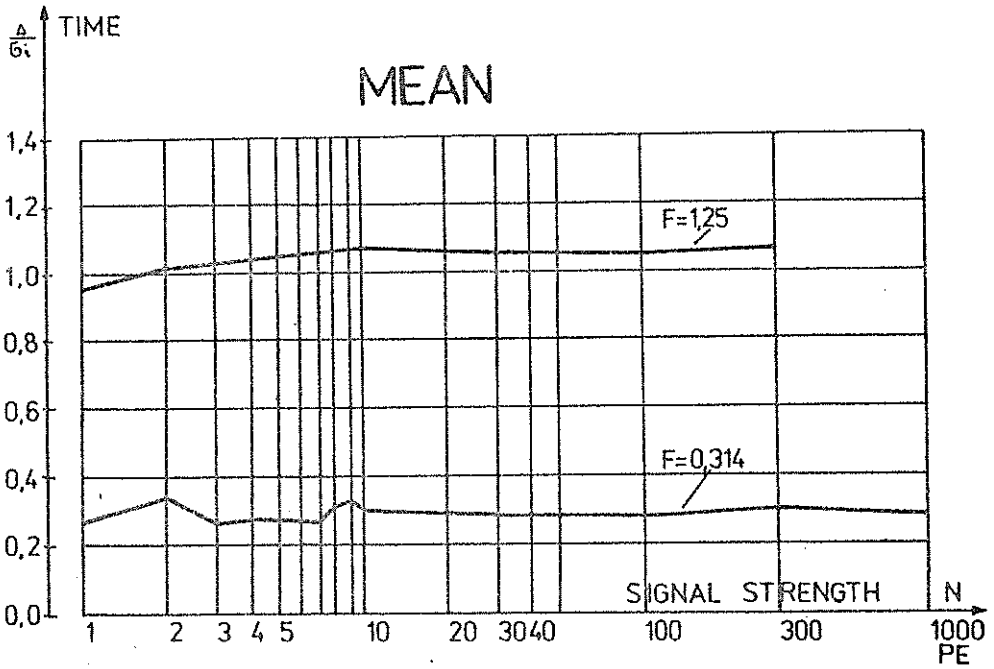

Fig.5. Mean value of result vs energy-half area case

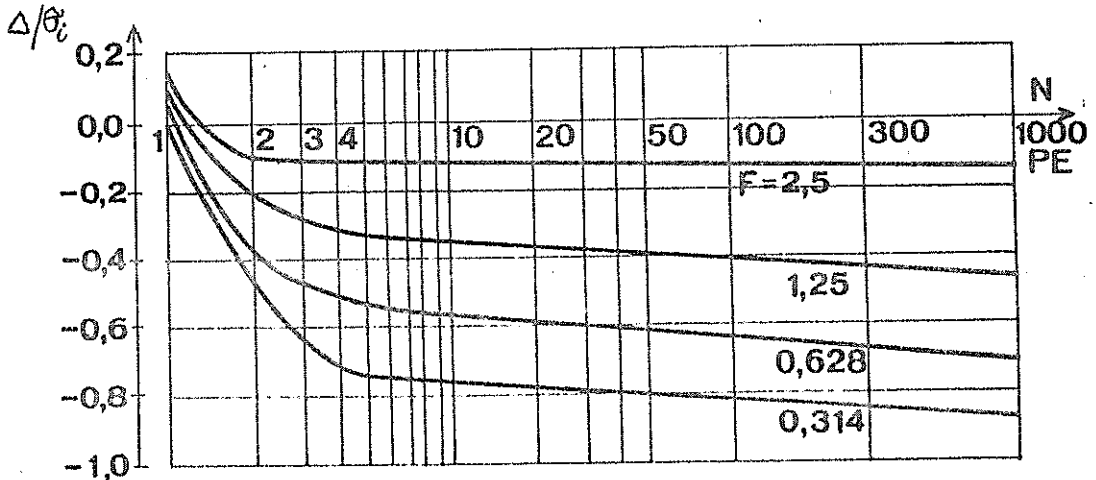

Fig.7. Mean value of result vs energy - c.f. case, f=0.5

TABLE 1

g coefficients, obtained experimentally

Fraction	Filter \ Signal energy /PE/	6	10	20	310
f=0.5	TF	1,61 /80/	1,45 /80/	1,27 /80/	1,34 /100/
	3PF , F=1.25	1,59 /180/	1,86 /220/	1,57 /260/	1,26 /100/
	3PF , F=2.5			1,32 /80/	
	3PF , F=3.75			1,20 /40/	
f≈1	TF	1,52 /40/	1,30 /40/	1,38 /240/	
	3PF , F=1.25	1,41 /60/	1,85 /100/	1,85 /300/	

g values

Filters: TF-11-section transversal filter matched to the logarithm of the signal shape.

3PF-3-pole RC filter of different filtration coefficients F.

Fraction f≈1 was obtained via zero-crossing detection in filtered and differentiated signal

Sample sizes are given in parentheses.

THERMAL EFFECTS ON DETECTORS AND COUNTERS

S. Leschiutta, S. Marra, R. Mazzucchelli,
Politecnico di Torino
Dipartimento di Electronica
Corso Duca degli Abruzzi, 24
10123 Torino Italie

Telephone 11 539 162
Telex 220646

ABSTRACT

With the centimeter accuracy approaching, also the minor uncertainty sources, such as the thermal effects on time discriminators and counters must be investigated. The behaviour of some of these devices is investigated experimentally and some results are presented.

THERMAL EFFECTS ON DETECTORS AND COUNTERS

1 Introduction

The laser ranging technique is now approaching the subcentimeter accuracy level and conseguently also the minor delay sources must be investigated.

This paper aims mainly to the thermal effects encountered in timers and time discriminators.

For the counters, the investigation was perfermed on the HP5370A device, that finds widespead use in laser ranging stations for its truly remarcable resolution of 20 ps. As time discriminators, a number of circuits were investigated, the final choice being the so called "centroid" type. In the following section the technical set up will be briefly described, while the third is devoted to the results. During these investigations also some amplitude effects and noise levels were measured and some relevant results are pointed in the fourth section. In the last, some conclusions are presented, along the planned future measurements.

2 Measurement system

The set up is depicted in Fig. 1; for the time discriminators, that can be operating outside of a building, the temperature range was -20 to +50°C; for the counter, that usually is kept in a shelter, the range was +12 to +30°C.

The temperature gradient was particulary controlled in the case of the counter, being of about 1°C/20 min, in order to allow a smooth variation of the temperature inside the device. The instrument was kept in the middle of the thermostatic chamber and a baffle was provided to shield the device from drafts coming via the conditioning system. The room in wich the testing equipment was operating, remained +1°C during the operations; sufficient time was allotted in order to reach a thermal equilibrium for all the instrumentation.

3 Results

3.1 Measurements on the counter

Two HP5370A (serial 1848A00413 and 2213A01367) were tested, with similar results; the reader is anyway warned not to extend the hereinbelow given results to other instruments of the same model, also if it seems that similar behaviours were encountered in other laboratories(1).

Since the "start" and "stop" levels can be set indipendentty via the computer, a number of measurement runs were performed at each temperature, changing the levels by steps of 50 mV, in the range 0.2 - 0.4V. The test pulse used was of 0.5V amplitude with a risetime of 2V/ns.

As a general rule, at any start and stop level, (also if different for the two channels), the counter readings increase with the temperature; this variation is roughly proportional to the temperature. There is additional evidence that, in the two instruments inspected, both levels rise with the temperature, albeit with a slight different slope.

In the particular case of same start and stop levels, the results are given in Fig. 2. The slope increases regulary with the level, and at 0.4V, shows a value of about +10ps/C°.

For any combination of trigger voltages and counter temperatures, no significant variations were observed in the fluctuation of the results, being the one-signa value around 20-25ps.

3.2 Measurement on a "centroid" time discriminator.

The time discriminator used for the temperature effect

measurements is a centroid device (2) that was presented at the 4th Workshop on laser ranging istrumentation. The circuit, with its delay line (a length of coaxial cable), was inserted in the chamber, mounted in a box, with the lid closen or open. The results are given in Fig.3; the delay slope, in the region from -20°C to +50°C, is of about -10ps/°C. In the range +15 to +25°C, the variation amounts to 120ps. With open or closed box the slope is the same, with a difference of some 150ps (Fig. 3).

It must be stressed that no particular selection or ageing of the components was previously performed.

Also in this case no significant variations were found in the fluctuations, as can be seen in table 1, in wich the absolute delay and the one-sigma standard deviation are given versus temperature; for each value, 10^3 measurements were averaged.

TABLE I

DELAY AND FLUCTUATIONS VERSUS TEMPERATURE
CENTROID DETECTOR

TEMPERATURE °C	-20	-10	0	+10	+20	+30	+40	+50
DELAY ns	6.387	6.222	6.130	6.047	5.986	5.801	5.791	5.698
STANDARD DEV. ps	27	26	25	24	25	26	25	22

4 Noise and amplitude effects on time discriminators

Three time discriminators were investigate a commercial constant level (not constant fraction) circuit, an "integrator" detector (3,4) and the abovementioned centroid device.

All the discriminators, were fed by an avalanche diode, illuminated by a laser diode pulse generator (5) sending 1000 pulses per second.

Tests on counters

The short term stability of the counters was tested with measurements lasting from 10ms to 10s.Fixed settings (1.5V) were used both for start and stop channels, that were driven via fixed delay lines from the same TTL pulse. The results for the fluctuations (one sigma values) and the relevant standard deviations (again one sigma) are given in table II.

TABLE II

COUNTER TIME STABILITY
duration of measurements seconds

	0.01	0.1	1	10
fluctuations ps	19.5	19.3	19.3	19.4
stand. dev. ps	1.35	0.47	0.1	0.1

No apparent drift is evident and the steady reduction of the standard deviation with the square rooth of time between 0.01 and 1s means that in this region we are confronted with a whithe noise process.

As regards the average fluctuations versus the pulse amplitude, the time proven rule to use settings just above half of the pulse amplitude was generally confirmed. For instance, with a trigger level of 1.5 V, the fluctuation drops sharply from 30-40ps to about 20ps, when the pulse amplitude crosses 3V.

A closer look to this behaviour has shown that, with fixed pulses and variable start and stop settings, the delay fluctuation is a non-monotonic function of the settings. This pattern depends from the pulse shape and from the individual counter and it is fairly constant. To quote some figures, with a 5V pulse and the stop level at 2.5V, the variation of the delay (one sigma value) ranges from 18 to 35ps, when the start level is changed from 1 to 4.5V. Conseguently it can be recommended to investigate for each individual counter, the "best" combination of pulse amplitudes and trigger settings.

As previously mentioned, the time discriminators were driven by an avalanche photo detector,illuminated by a solid state laser. Three devices were tested: A, fixed level discriminator; B, integrator; C "centroid", with a fixed delay line. The delay of each circuit, in nanoseconds, and the fluctuations (one sigma) in picoseconds are given in table III, for measurement durations from 0,1 to 100s.

The absolute values of the delays are of no concern, since they depend from the specific values of the circuitry; the attention is called on the variations, with time, of the delay, that anyway can be disregarded for all three circuits. The performances of the circuit A (fixed trigger levels) is remarcable,

but this solution is quite sensitive to signal amplitude variations.

Changing the slope of the electrical pulse driving the laser from 1.8 to 3.1ns and keeping constant the energy, the variations in fluctuation for circuits A and C, are less of 1ps and for circuit B of about 6ps. Conseguently discriminator B is more sensitive to e shape of the pulse.

TABLE III

TIME STABILITY
Duration of measurements-seconds

CIRCUIT		0,1	1	10	100
A	ns	5.428	5.428	5.428	5.428
	ps	16.8	16.7	16.9	17
B	ns	1.842	1.848	1.852	1.846
	ps	28.5	29.7	29.4	29.2
C	ns	6.116	6.120	6.125	6.130
	ps	23.4	24.8	24.6	24.1

5 Conclusions and programs

From the above given results it seems that the "centroid" time discriminator is well adapted for the timetagging of the departing pulse in laser telemetry stations.

The time walk can be disregarded for calibration intervals up one hour, but the temperature of the time discriminators and counters must be kept under strict control if the 100ps accuracy region must be reached, since some of these devices are affected by temperature effects of 10ps/°C.

As regards the future developments, similar tests will be performed on preamplifiers and on commercial "constant fraction" discriminators.

Torino, November 1984

References:

1) Dr. D. Kirchner, Graz Technical University, private communication.

2) J.F. MANGIN: The laser and the calibration of the CERGA lunar ranging system. 4th Int. Workshop on laser ranging intrumentation, vol. 2, p. 162-165, 1982.

3) A.B. SHARMA, S.J. HALME. Receiver for laser ranging to satellites IEEE. Trans. Instrum. and Measur., vol IM 30, p. 3-7, 1981

4) A.B. SHARMA: An Integrating, Centroid Timing Receiver for Satellite Ranging, Reports of the Finnish Geodetic Institute 75:10.

5) Y. TSUCHIYA, A. TAKESHIWA, M. HOSODA: Stable ultrashort laser diode pulse generator. Rev. Sci. Instr., vol. 52, p. 579-581,1981.

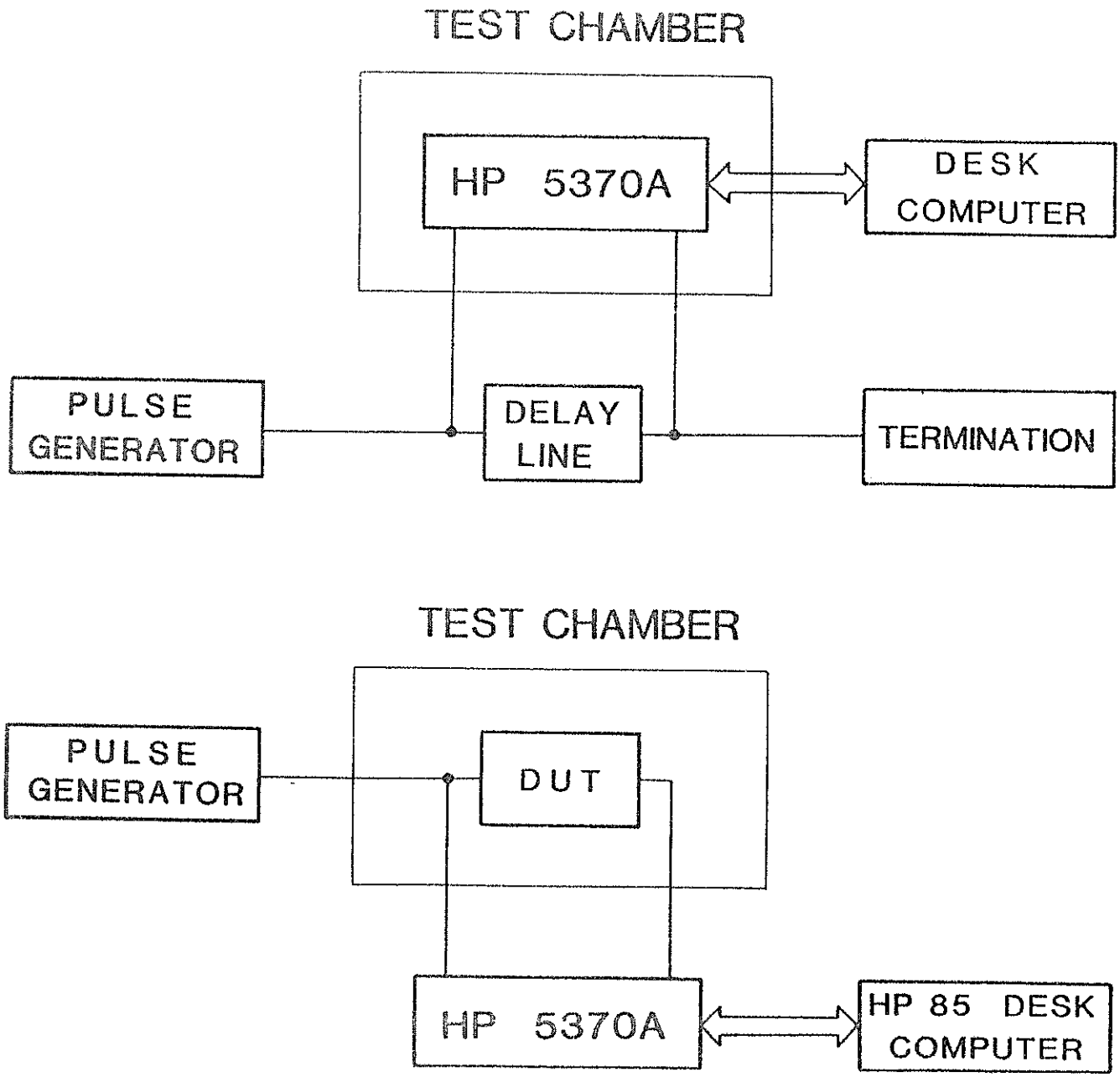
TEST CHAMBER
HP 5370A
DESK COMPUTER
PULSE GENERATOR
DELAY LINE
TERMINATION
TEST CHAMBER
PULSE GENERATOR
DUT
HP 5370A
HP 85 DESK COMPUTER

FIG.1

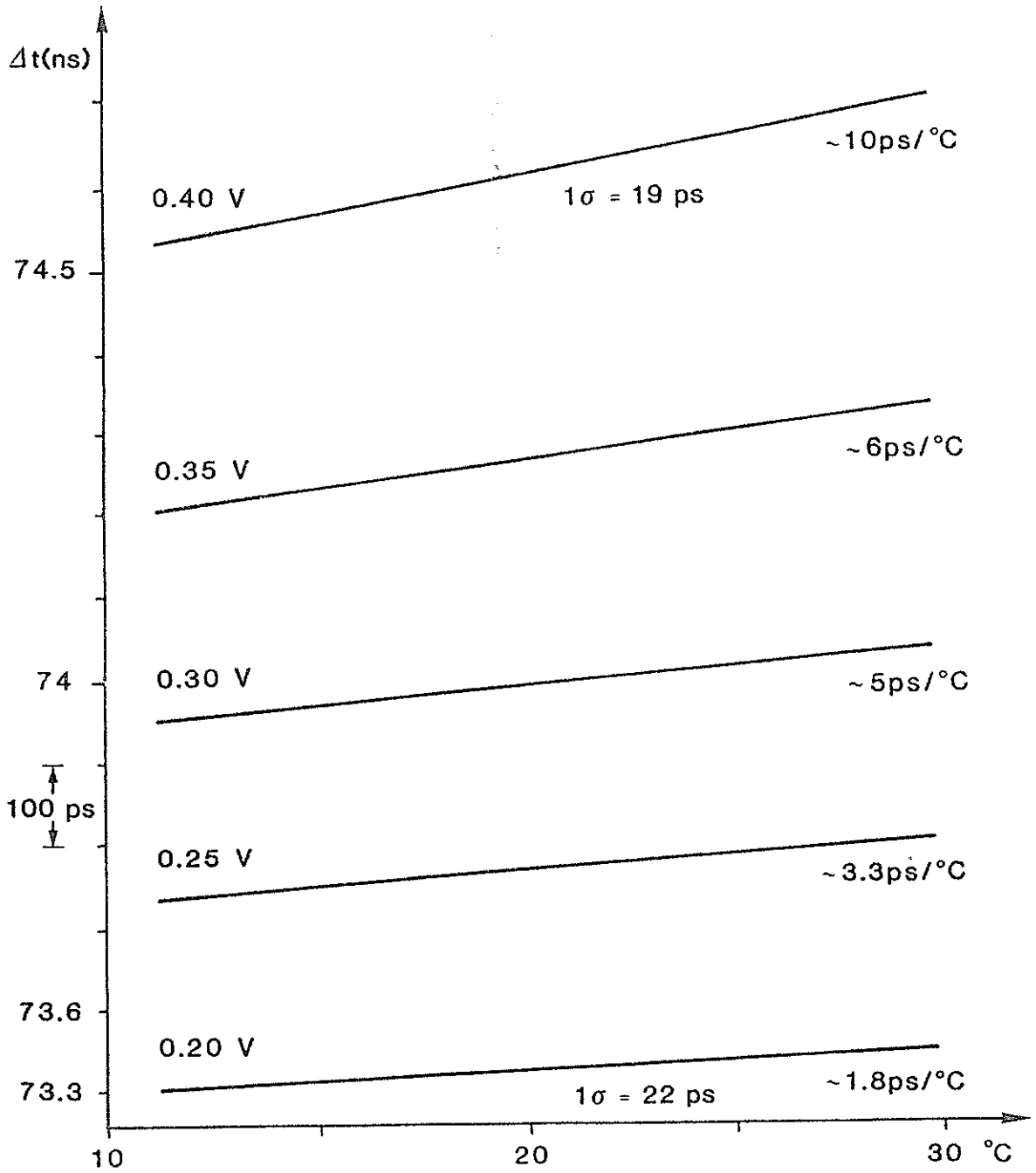

SAME START AND STOP LEVELS

FIG. 2

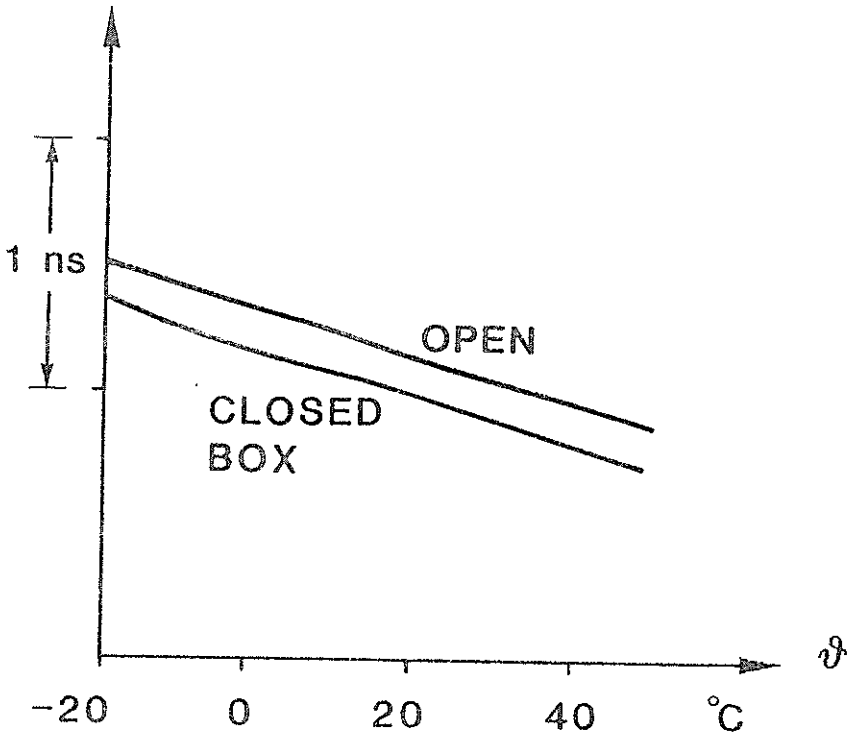

FIG. 3

FURTHER THOUGHTS ON A MINIMAL TRANSMITTER FOR LASER RANGING

B. Hyde
Alp Optics
267. Rue du Château du Roi
38220 Vizille France

Telephone (76) 68 24 05

ABSTRACT

It has been suggested that it is advantageous to utilise the fundamental wavelength for satellite (or lunar) laser ranging. This has the merit of better atmospheric transmission etc.. and consequently a simpler laser system. A major objection was the P.M.T. required. In this paper, we exploit the high quantum efficiency of the triggered avalanche detector (TAD), which appears to answer this critisism, and using the more rigorous approach, recalculate the minimal transmitter requirements for, for example, LAGEOS at 1,06 µm. To further the raliability of the laser, we also introduce an automatic peak power limiter of simple form.

Further Thoughts on a Minimal Transmitter for Laser Ranging.

Introduction.

As third generation systems reach maturity and become widespread,it is instructive to review their fundamental design, with new technology in mind,and make recommendations for future Instruments and updates of existing ones.

A third generation system as implemented at present, has,typically,an emitter producing a single pulse of 30mJ,100pS, at 532nM and 10Hz,with a receiver which detects single photo-electrons.(P.Sharman,SLR Technical Note No. 1,MAY 1982, Roval Greenwich Observatory)

These systems are sub- optimum,as discussed at Lagonissi and there would seem to advantages in reviewing the suggestions presented there.(Proc. of the Third & Fourth Int. Workshop, 1978 & 1981).

Recapping,these were;

a) Detection by single photo-electron counting.
b) Using the mode- locked train of pulses.
c) Transmitting the fundamental wavelength(1064nM).

The first recommendation is now in common use.The second idea is sound but has not been popular or necessary given the large laser pulse energy available. The final idea was impractical for lack of a suitable photon counter in the near infra-red.

Our purpose in this paper is to quantify these advantages of using the intrinsic properties of the laser,and by means of a solid-state photon detector of high quantum efficiency,indicate how this may be done.

Advantages.

A quantitative 'feel'for the benefits of the aforementioned suggestions can be gleaned from a system budget. (figure.1)
Here we present the maximum and typical performance of a current system,relative to that of a proposed system emitting and receiving photons as a mode-locked train of pulses. An Instrument can be improved in this way by up to two orders of magnitude,dispencing with two lossy laser components and introducing a solid-state detector.There is also a gain in atmospheric transmission at the longer wavelength,dependant upon local visibility,elevation angle and station altitude. (R.I.HYDE,D.G.WHITEHEAD,Proc. of the Fourth Int. Workshop, Vol.1 pg. 251).

On the debit side the noise count increases due to dark noise of the detector and one should note the increase in the diffraction limited beam divergance.These are not normally limiting factors of an instrument.

There is a tacit assumption that the radar cross-section of the cube- corners is similar at both wavelengths.

On balance the gain of two to three orders of magnitude will manifest themselves in reliability, transportability and cost.Instrument downtime is normally dominated by laser reliability.

Implementation.

Photon counting is a well established and precise detection technique when one ensures 'singles' so avoiding discriminator non-linearity.To date it has been limited to the visible and ultra- violet wavelengths,so necessitating second harmonic generation.

Detection ,with internal gain,in the near infra-red is limited by 'excess noise'. The recent use of such detectors in a pulsed mode demonstratedthat they could detect single photons for a small but acceptable period of a duty cycle.

The identification of a return from a train of pulses requires a decoding procedure,but given the precise interval between each pulse, it is possible and has been used by E.C.Silverberg et al on TLRS-1.

FIG.2 Minimal Laser Energy versus Solid Angle.

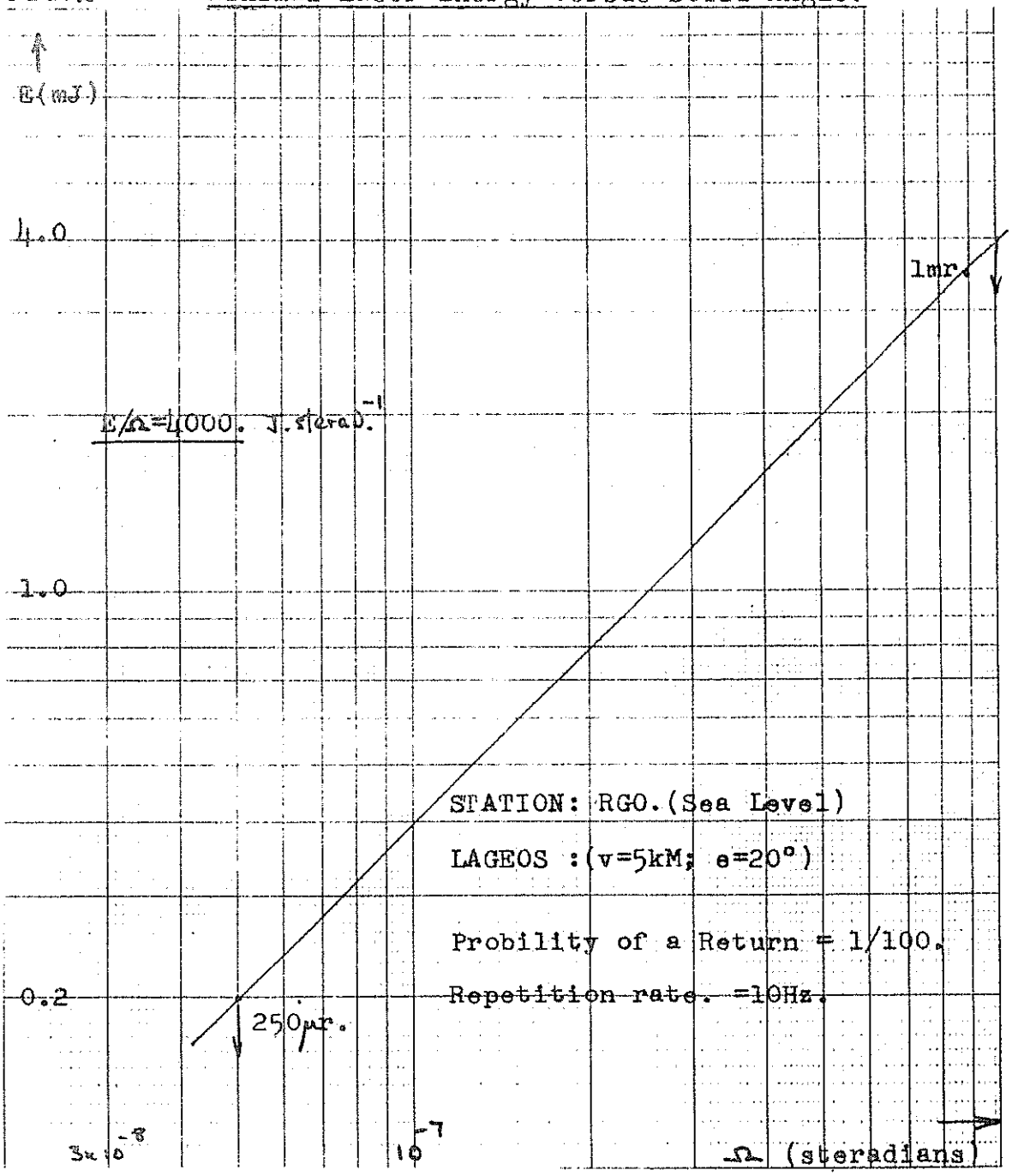

The Triggered Avalanche Detector.

In its continuous mode the avalanche photo-diode is unable to detect signals of less than 100pe. Recently a regular APD was operated in a pulsed mode and was able to detect single photo-electrons,during part of its duty cycle.

This work was reported by P.A.Ekstrom,J.App.Phys. 52(11),Nov.1981,pg.2013, and was followed up by work done by T.E.Ingerson et al ,App.Optics,vol.22, No.13, Silicon devices are now available commercially.

Our interest,here,is in the near infra-red,and therefore with a germanium device.Although germanium is not conducive to avalanche detection 'TAD operation is favoured by large and equal ionisation rates.' Ekstrom concludes his paper thus.'germanium should be an excellent material for TAD fabrication extending the ability to count photons to 1.5micro-meters.'

With such a device the following specification would be expected.

Quantum efficiency.	0.5
Gain.	1.exp(9)
Response time.	0.1nS
Enable period.	0.1S
Turn on delay.	200nS
Dark noise.	1.exp(5)/S at 77°K.

Minimal Energy Required.

It is instructive to estimate the minimal laser energy for the SLR system proposed.Using the parameters of the RGO instrument we determine that the minimum radiance of 4000Joules/steradian is required to range to Lageos in marginal conditions.
Figure 2. is a plot of minimal energy againstthe emitted beam solid angle.We see,for example,that with a beam divergence of 1mradian the minimal laser energy is 4mJ. i.e.within the compass of an unamplified oscillator. (Extrapolation to Lunar operation with a 30microradian beam at 10° above the horizon indicates a minimal of o.1J).'

Conclusion.

The intrinsic properties of the laser and in particular the mode-locked laser may be utilised more effectively.

To summarize,these properties are;

The near infra-red wavelength.

The mode-locked output format.

A unique polarisation.(e.g.see D.Curry et al, Proc. of the Third Laser Workshop.)

A 'clean' wavefront.(to avoid wavefront noise in the latter pulses of a train,see Spectroscopy Letts.8(5),329-340, 1975.R.B.Weisman etal.)

Finally,to implement them,to use the germanium TAD.

The advantages may be as much as three orders of magnitude,enabling one to operate without YAG amplifiers and a pulse switch out unit.

A retrospective update can be carried out during a regular service interval.Reliability and financial advantages follow.Other positive factors are eye-safe operation and mobility.Lunar systems can also benefit.

Clearly it is necessary to prove the germanium TAD but lasers of Ruby or Alexandrite can use the silicon device.

'.....you have nothing to lose but your chains'. (Marx.K.)

System Budget

FIG.1

STAGE	MAX.	TYP.	PROP.	COMMENTS.
0.Oscillator.	1	1	1	-
1.Swich-out.	1/3	1/10	1	transmit whole train.
2.Ampl.gain.	G	G	g	
3.Harmonic genr.	1/4	1/6	1	no photon conversion.
4.Detector q.e.	2/3	1/5	1	germanium TAD.
	G/18	G/300	g	factor 18 to 300.
Atmos. Trans.				
5a).v=25kM. e=90°.	2/3	2/3	1	
5b).v= 5kM. e=20°.	2/35	2/35	1	factor of 5000 max.
Noise.				
6a).Backgrnd.	2/3	1/5	1	high q.e. of TAD.
6b).Dark noise.	1/2	1/2	1	

A PICOSECOND STREAK CAMERA FOR SPACEBORNE LASER RANGING

W. SIBBETT, W.E. SLEAT
Blackett Laboratory, Imperial College
Prince Consort road, London SW7 2BZ ENGLAND

Telephone 01 589 5111
Telex 261503

W. KRAUSE
Messerschmitt-Bolkow-Blohm GMBH,
Postfach 801169
D-8000 München 80, WEST GERMANY

Telephone 089 6000 4093
Telex 5287370

ABSTRACT

Pertinent details relating to the design, construction and preliminary evaluation of an experimental circular-scan streak camera are presented. This "Photochron IIC" picosecond camera is intended as a major subcomponent of a spaceborne laser ranging instrument. Experimental data are included which confirm that an instrumental function of less than 6 ps can be achieved in both single-shot and repetitive modes of streak operation

A PICOSECOND STREAK CAMERA FOR SPACEBORNE LASER RANGING

1. INTRODUCTION

A spaceborne ultrashort-pulse laser ranging system may be employed to determine with high accuracy the distance from an artificial earth satellite to ground-based retroreflector targets. (1, 2) The laser ranging instrument essentially comprises a laser which emits picosecond pulses at a repetition frequency of 10-20 Hz, transmitting and receiving optics, a detector and some means of measuring the round-trip time between the satellite and retroreflector. Provided a correction is made by which the pulse retardation arising from atmospheric refraction is taken into account, then this round-trip time can be translated into a measurement of the straight-line distance. However, this atmospheric correction is computed from a theoretical model of the atmosphere that requires knowledge of the atmospheric surface pressure at each target site. An elegant method of obtaining such surface pressure data consists of deriving them from differential pathlength measurements carried out simultaneously at two or more laser wavelengths (3).

The general concepts for a modern two-colour spaceborne laser ranging system have been reviewed by Lutz and coworkers. (2) In this, the time-interval measurement unit is based on a circular-scan streak tube (4,5) operating in a "vernier" mode. This means that in order to measure the round-trip transit time, complete periods at the scan frequency that elapse between the start and stop pulse registrations are counted by a "coarse" counter and the fractional period is recorded with high precision at the output screen of the streak tube. (2,6) An experimental "Photochron IIC" streak camera is being developed for such a spaceborne differential ranging application in conjunction with fundamental (λ750nm) and second harmonic (λ375nm) picosecond pulses from a vibronic (eg alexandrite) solid-state laser. The specialised features of the Photochron IIC will be described and data will be included which relate to preliminary evaluations of its temporal resolution capability when incorporated in an experimental camera format.

2. CIRCULAR-SCAN STREAK CAMERA PRINCIPLE

The basic component of any electron-optical streak camera is the image tube and although several tube configurations exist the general principles of their operation have a lot in common. Before discussing the circular-scan version it is perhaps worthwhile reviewing the concept and operation of linear-scan, single-shot and repetitively-operating modes.

2.1 Single-Shot Operation

A conventional single-shot modular camera system which comprises a Photochron II (7) streak tube is illustrated schematically in figure 1. For the sake of clarity, suppose

that two temporally separated reflections of a single ultrashort pulse are produced by a glass disc of known thickness. These illuminate a slit which is imaged onto the photocathode by an appropriate input relay lens. The length of the slit image is typically a few mm at the cathode where its height is arranged to be less than the width of one spatial resolution element. A photoelectron replica of each incident transient slit image is then produced promptly ($<10^{-13}$s) at the cathode. However, it is at this initial stage that one of the primary contributions to the limiting time resolution of the streak tube becomes evident. This is that the electrons are liberated from the cathode with a distribution of energies and angles. Consequently, the spatial and temporal confinement of the electron image very near the cathode surface would rapidly degenerate with propagation and in the time dimension this is usually referred to as photoelectron transit time dispersion. The energy spread of the photoelectrons is a function of both the wavelength of the incident radiation and the cathode spectral response characteristic and therefore when these parameters are preselected it is then necessary to ensure that the transit time dispersion is minimised. To do this, a mesh electrode is placed close to the photocathode so that a high "extraction" electric field can be applied to enable the low energy (usually < 1eV) emitted electrons to rapidly reach relatively high energies (> 1keV) such that they achieve high velocity before significant spatial separation has occurred. Appropriate voltage applied to suitably shaped cone and anode electrodes complete the focussing electron-optical lens which constrain the photoelectronic signal to pass through a small anode aperture. This geometry thus effectively decouples the electron-lens from the deflection and subsequent field-free (or drift) sections of the streak tube. (The accelerating potential maintained on the anode and phosphor screen (or equivalent) is generally 15 - 20KV for this type of arrangement). When no electrostatic deflection is applied, then the two ultrashort electron slit images would be

focussed onto the phosphor screen where they would be super-imposed with the so-called "static" (or "focus") spatial resolution of the image tube.

Temporal resolution is afforded in a single-shot "streak" (or "dynamic") mode of operation. To achieve this, a bias voltage is applied to the deflectors so that the electron signal is prevented from reaching the screen within a prescribed detection area. An appropriately synchronized linear, time-varying voltage differential is then applied to the deflectors (either symmetrically, ie + V to one plate, - V to the other, or asymmetrically) so that the electron packets experience a deflecting electric field as they travel through the deflection region. The transient and temporally separated replicas of the incident optical slit images are thus displayed on the screen with a displacement separation that depends on the rate of change of applied voltage. A time-to-space transformation has therefore been accomplished in the streak image tube.

In the example which is depicted in figure 1, the streak image has in inbuilt time calibration because the glass disc was of known thickness. It follows, therefore, that when the width (FWHM) of the intensity profiles of the streaks is determined (directly from photoelectronic recording) this can be related to the temporal separation to provide the so-called recorded streak duration, δT_R. When gaussian pulse shapes are assumed then the relationship connecting δT_R and the incident pulse widths δT_p is given by:

$$\delta T_R = \{(\delta T_p)^2 + (\delta T_{phys})^2 + (\delta T_{tech})^2\}^{\frac{1}{2}} \quad (1)$$

δT_{phys} and δT_{tech} are the main contributing factors that determine the limiting time resolution (often referred to as instrumental function) of the streak tube and refer

respectively to the transit time dispersion of the photoelectrons in travelling from the cathode to the deflectors and the streak limited time taken for the electrons to be swept across one resolution element at the screen. These so called physical and technical contributions can be expressed in the form given in equations (2) and (3)

$$\delta T_{phys}\ (ps) = \frac{23.4(\delta\varepsilon)^{\frac{1}{2}}}{E} \qquad (2)$$

where $\delta\varepsilon$ is the FWHM (eV) of the energy distribution of the initial photoelectrons emitted from the cathode and E (in KV/cm) is the applied electric field strength close to the cathode. (Other factors which contribute towards δT_{phys}, for example pixel aperture size effects, are excluded in this context. Information is considered only as far as the screen of the sheet image tube).

$$\delta T_{tech}\ (ps) = \frac{10^{11}}{v\delta} \qquad (3)$$

where v is the streak velocity (cm/s) at the screen and δ (line pairs/mm) is the estimated spatial resolution under streak conditions. (It has been recently shown in theoretical studies (8, 9) of Photochron streak tubes that the evaluation of the instrumental function according to equations (1)-(3) is rather too simplistic. δT_{phys}, as given, really only refers to the photo-electron transit time dispersion in the cathode-to-mesh region whereas a proper treatment includes all the regions between the cathode and deflectors. Moreover, a better method (9) for estimating the overall camera resolution which involves a temporal modulation transfer function has been suggested. In this more physically realistic approach, account is taken of the interactive aspects of acceleration, focus and deflection. However, in the context of the present consideration, where

an instrumental function of several picoseconds is involved, then the approximate estimates deduced from equation (1) - (3) are adequate).

It must also be pointed out that it is usually not possible to draw sufficient photocurrents in picosecond streak tubes to provide streak intensities at a recordable level in single-shot operation. This arises because space charge effects give rise to severe degradation in both spatial and temporal performance (8). As a result it is commonplace to employ externally (or internally, see section 3.2) coupled high-gain intensifiers. The fact that the temporally dispersed data are displayed on the streak tube as a spatio-intensity variation, determines the requirements of the intensifier to be (i) high signal gain and (ii) good spatial resolution with minimal image distortion. The intensified output is then generally recorded photoelectronically or photographically.

It has already been demonstrated experimentally that an S20 Photochron II single-shot streak camera having a lens-coupled, magnetically focussed intensifier can have a limiting time resolution of just less than 1ps at a wavelength of 735nm (10). Also, an S20 Photochron II camera which incorporated a fibre-optically coupled channel-plate intensifier has been demonstrated to have an instrumental function <2ps for an incident wavelength of 605nm (11).

2.2 Repetitive (or Synchroscan) Streak Operation

When the incoming luminous information has a moderately high repetition rate (>MHz) then a synchronous streak operation can be exploited (12). The basic concept is indicated in figure 2 where it can be seen that the applied sinusoidal waveform provides a synchronised repetitive electrostatic deflection. The central half amplitude of the sinusoid is linear to within 5% and provided there is little or no

relative jitter between the incident light signals and the deflection voltage waveform, then all of the streak images can be superposed on the streak tube screen. A direct result of this scheme is that many weak individual streaks can be integrated in intensity to achieve a recordable output signal level without the need for an image intensifier while still avoiding space charge effects. The streak images, however, have a recorded width which also includes any jitter component and so the instrumental function must be expressed as:

$$\delta T_{instru} = \{ (T_{phys})^2 + (T_{tech})^2 + (T_{jitt})^2 \}^{\frac{1}{2}}$$

where δT_{phys}, δT_{tech} are as explained in section 2.1 and δT_{jitt} is the additional limitation arising through jitter.

Photochron I, II streak cameras operating synchronously at repetition rates of 140MHz and 165MHz have been demonstrated to have time resolutions < 10ps (13 - 15). More recently, an improved design of the Photochron II which has been designated as the "Photochron IIA" has been operated in the synchroscan mode and the results show that the instrumental function is 1ps (16), which implies that the jitter contribution is relatively small.

2.3 Circular-Scan streak Operation

For the purposes of laser ranging it is convenient to have a circular-scan streak (4 - 6) of constant period so that no synchronization requirements arise. The basic operation is single-shot in nature but the electrostatic time-varying deflection is established by the application of two RF sinusoidal voltages in phase quadrature and so this scheme combines many of the features mentioned in the two previous subsections. It is distinct in that the voltage sinusoids are supplied to two sets of deflectors which produce

orthogonal electric fields with a $\pi/2$ phase difference so that a circular trace is produced at the screen or equivalent plane. When the period of this continous scan is T(in ns) then the technical resolution limit may be expressed as:

$$\delta T_{tech}\ (ps) = \frac{100T}{\pi d S}$$

where d is the diameter of the circle (in cm) and S is the spatial resolution (in lp/mm) under the streak conditions. The expression for the photoelectron transit time dispersion (δT_{phys}) remains the same as that already given in equation (2).

Clearly it is necessary in this approach to use a point image on the photocathode rather than an extended slit format and since a single picosecond pulse is selected from the laser at a low repetition rate (~20Hz) then image intensification must be retained. The experimental circular-scan Photochron IIC streak camera which has been designed specifically for this type of operation is described in the following section.

3. CIRCULAR-SCAN "PHOTOCHRON IIC" STREAK TUBE

The design of the circular scan streak image tube, designated as "Photochron IIC" is shown schematically in figure 3. The defining areas of electron manipulations are; (a) the electron-optical lens constituted by the photocathode K, mesh M, focussing cone C and anode A, (b) the deflection section comprising orthogonally oriented pairs of deflectors placed on each side of a "screening" aperture plate; and (c) a field-free drift section terminated by a proximity-focussed high gain microchannel plate (MCP) intensifier where the electron image is directed onto a phosphor screen (S) deposited on a fibre-optic faceplate (F).

3.1 Electron-Optical Lens Section

A semitransparent S20-type (Na-K-Cs-Sb) photocathode was processed on a specially profiled substrate such that a usable diameter of 10 mm was provided. The available spectral ranges of sensitivity extend over the 300 - 900 nm region and easily accommodates the 760 nm, 380 nm optical pulse wavelengths to be used in ranging systems. When illuminated by pulses at these wavelengths, the photoelectrons emitted from the cathode have an associated energy distribution. As already pointed out in subsection 2.1 it is necessary to minimise the transit time dispersion that accrues as the electron packet travels towards the deflectors, so a planar mesh electrode is placed 0.5 mm from the cathode such that the electrons rapidly reach an energy of approximately 1KeV. This is arranged by maintaining a dc EHT voltage of -15kV on the cathode and -14kV on the mesh. The mesh to which is applied this so-called "extraction" potential is fabricated in thin copper from which a high density of "cells" or windows have been etched. (The cell density is 300 cells/cm and the transparency is 50%). It is ensured during construction that good surface contours exist in this region of high electric field (20kV / cm) so that the incidence of "field emission" is eliminated.

The imparted energy of 1KeV to the electrons transmitted through the mesh electrode is sufficiently low that a photoelectronic image can be focussed in the plane of the input face of the microchannel plate using the "singlet" electron-lens obtained by supplying an appropriate combination of voltages to the mesh M, cone C and anode A electrodes. (The anode and the input of the microchannel plate are maintained at the same potential). For the voltages already mentioned for the cathode and mesh, the typical operating potentials for the cone and anode electrodes are 13.45KV, 4.5KV respectively. Under these operating conditions the electron-optical magnification is

-1.8 (-ve signifies image inversion) and the limiting spatial resolution at the photocathode is in excess of 35 lp/mm. Although this spatial resolution can be retained in the sweep direction under conditions of repetitive or "synchroscan" streak operation (see section 2.2) the elevated current densities that arise in the single-shot streak mode lead to substantial reductions in this value. In fact, a typical estimate is 20 lp/mm at the photocathode.

The basic feature of this type of tube is that the electron lens provides moderate spatial resolution (in two dimensions) together with reasonably good retention of the temporal fidelity of a "transient" photoelectron slit object. The Photochron II (7) and Photochron IIA (16) version have achieved subpicosecond resolution (10,17) and therefore have adequate performance characteristics for the purposes of laser ranging applications.

3.2 Proximity-Focussed Intensifier Section

It has already been explained that an image intensification stage is necessary in a single-shot streak camera so that recordable image intensity levels can be produced without compromising the image tube performance through the space charge effects arising from enhanced photocurrent densities. An alternative to coupling an external image intensifier module is to incorporate an intensification stage within the structure of the streak tube. This is the design concept of the Photochron IIA tube where a high electron gain is offered by a proximity-focussed microchannel plate-to-phosphor section. The micro-channel plate comprises a matrix of 12.5μm diameter ratio of 80: 1 on a 15μm centre-centre spacing. The activated inside walls of the hollow channels have a suitably high secondary emission coefficient for the incident 10.5 KeV primary electrons and a cascade of secondaries is ensured by the multiple collisions within the confines of the microchannel plate (MCP). Forward momentum

of these secondaries is provided by the positive voltage bias (>1.5kV) applied between the output and input MCP faces. A gain 10^3 can be obtained in such a MCP which has a limiting spatial resolution of more than 25 lp/mm. In this type of intensifier, the creation of +ve gas ions can be a problem because their feedback, which is encouraged by favourable potential gradients, gives rise to serious induced "noise" levels. This shortcoming is alleviated by having a 15^o bias angle on the channels and a 20 nm aluminium oxide (Al_2O_3) layer on the input MCP face so that the penetration by primary electrons is permitted by the feedback of slow positive ions is suppressed.

There are advantages in this internal proximity-focussed intensifier scheme compared to the optically-coupled external intensifier arrangement that relates to the modular approach outlined earlier in section 2.1. For instance, the electron lens aberrations such as off-axis image distortions that exist in many "inverting" direct-viewing intensifiers are eliminated and inherent photocathode background noise associated with a separate intensifier tube is avoided. One possible disadvantage is, however, that picosecond electron signals are amplified in the internally intensified version in contrast to microsecond electron images (arising from the screen phosphorescence timescale) for the externally coupled counterpart and consequently gains saturation problems (18) may be exacerbated. Notwithstanding, subpicosecond resolution in single-shot operations has been measured for a Photochron IIA type camera (17). Another problem, arises from the feature that the open area ratio of the microchannel plates is 66% and the resultant loss of signal photoelectrons is damaging to the overall signal-to-noise ratio.

The intensified electronic image is proximity-focussed onto a suitable phosphor screen which is deposited on a fibreoptic output faceplate. For this purpose an accelerating potential of 3-5KV is applied between the exit face of the MCP and the

screen which have a separation of 0.8 mm. It is important that the properties of the phosphor screen are designed to be compatible with both the image tube and the read-out device employed.

To facilitate a spatial resolution parameter which does not limit the performance of the streak tube a fine grain phosphor power is a prerequisite where the grain size should be 1 - 2μm (19). The method of deposition onto the fibre-optic faceplate (6μm cores) is chosen so that a uniform layer thickness and packing density is obtained.

In the case of the CSST where the read-out device is a self-scanned photodiode array (RETICON) or CCD which have a peak detection efficiency at 800 nm, it is clear that a red phosphor should offer the best spectral match. However, it must be remembered that a high efficiency and good spatial resolution are needed to ensure an overall detection efficiency comparable with the alternative yellow-green (P20) phosphor screens that are presently available on commercial intensifiers.

The forward transfer of the luminescence towards the detector is enchanced by depositing a backing layer (50 nm thick) of aluminium onto the phosphor screen. This is arranged so that it can withstand the application of electric fields in excess of 40KV/cm in the proximity section. (The screen is generally maintained at earth potential).

3.3 Deflection section

To produce the desired circular sweep in the streak tube, two pairs of orthogonally oriented deflection plates are arranged as illustrated in figure 3. The design of the deflector assembly in the Photochron IIC lends itself to efficient coupling of power via metal-ceramic electrical feedthroughs which exhibit acceptably low RF losses. The dimensions and

separations of the deflectors have been chosen to provide equal deflection sensitivities and it turned out in practice that due to tube manufacturing tolerances the set nearer the anode required 211V for 1 cm deflection while the orthogonally oriented set had the slightly reduced sensitivity of 226V/cm. It is necessary therefore, to differentially adjust the suppplied RF power because of the importance of providing equal deflection amplitudes in phase quadrature. Failure to ensure this leads to ellipticity in the scan as illustrated in figure 4 where one amplitude is allowed to exceed the other by 2%, 4% and 6%. (Dotted outline of ideal circle is included for comparison).

The effect of any departures from precise phase quadrature is also indicated in figure 4 where the induced distortion in the scan is clearly evident for phases differences that are 2^{o}, 4^{o} and 6^{o} larger than the required $\pi/2$. The overall distortion in the circular scan that results from combined amplitude and phase drifts are also included in figure 4 and the correspondingly computed amplitude and phase errors are presented for a total scan rotation in figure 5. Both of these figures vividly confirm that the fidelity of the circular scan relies critically on keeping the amplitude and phase errors to a minimum during the operational period of the camera.

Our first practical attempt to satisfy the stringent deflection requirements for the Photochron IIC involved the use of an effective half wavelength of transmission line with the deflectors located at points of equal signal amplitude but $\pi/2$ out of phase. Unfortunately, the deflector capacitance was sufficiently dominant that this scheme behaved as two tightly-coupled tuned circuits with inevitable multiple resonances. Consequently, the simultaneous adjustment of resonance and phase proved to be impractical without the use of excessive power.

In the alternative approach, that is being used at present, a single amplifier is used to provide two independent drive signals. The two sets of deflection plates are coupled to the 50 ohm impedance signal lines by suitable coupling loops which are adjusted to provide a matched load. To minimise the influence of phase drift resulting from induced thermal effects, the two circuits are appropriately damped and phase adjustment is made by slight alterations to the cable lengths. As mentioned earlier, our experimental streak tube has sets of deflectors that differ by approximately 7% in sensitivity but this was overcome by a suitable amount of resistive damping.

The sinusoidal deflection voltages are produced by a 300 MHz crystal controlled oscillator, figure 6 or for synchroscan operation a laser driven tunnel-diode oscillator. The signal is further amplified by a wide band amplifier (Model TRW-CA2820) to give an output of 400 mw into a 50Ω load. For practical demonstration of a 3 cm diameter circular scan further amplification is required. An appropriate amplifier module was obtained (Microwave Modules Ltd) which is capable of continuously delivering 30 watts of RF power without requiring a precisely matched load.

The actual power used in experiments to date is approximately 15 watts total. This power and damping has proved to give satisfactory stability to enable mutual evaluation of the CSST time resolution (20) to proceed and produced a circular scan having a diamter of 30mm at the phosphor screen. A photograph of such sweep, for a continuous light surce, is reproduced in figure 7.

As well as amplitude variations on the circular scan it must be remembered that an absolute ranging measurement relies critically on exacting frequency stability. In fact, if a loss of 1 ps time resolution is to be avoided then the frequency stability should be better than one part in 1.5 x

10^{10} during the 15ms double-transit time. This could be satisfied by basing the 300 MHz oscillator on a Rubidium clock frequency standard rather than the quartz crystal specified for this study. An additional constraint is that the circular orbit of the electron beam must remain centred at the same point to ensure appropriate detection and so it follows that influences such as stray magnetic fields must be avoided.

4. THE PHOTOCHRON IIC CAMERA AND ITS DYNAMIC PERFORMANCE

In our laboratory camera arrangement the input optics to the streak tube comprised a 20 μm diameter pinhole which was imaged, with a X2 demagnification by a relay lens on to the photocathode. The streaked output images were recorded photographically on Ilford HP5 film using an f/1.5 lens operating at a magnification of unity. A crystal-controlled oscillator/multiplier network (21) produced a power of 400 mW at 300 MHz which was subsequently amplified to approximately 15 W before being appropriately shared in phase-quadrature between the sets of deflectors. This was accomplished by supplying the RF signals to the tube via $\lambda/4$ matching transformer and two 50 ohm impedance coaxial cables that differed in length by one quarter of a wavelength. These cable outputs were then loop-coupled to the deflection plates, the loops being adjusted to give matched loads. Although we have already demonstrated that a 30 mm diameter scan can be obtained with as little as 2.5 W of power in each feed channel (21) we chose to supply higher power levels, in this instance typically 5 - 10 W per channel, to lower Q tuned circuitry. By this means it was possible to reduce drifts in signal phase and hence maintain the fidelity of the scan and also have a better mechanical arrangement for the resonant circuits. (The importance of maintaining relative phase together with the necessary avoidance of appreciable amplitude variations to the orthogonally oriented pairs of deflectors has already been alluded to (section 3.3).

As has been stated earlier, an estimate of the instrumental function of this Photochron IIC camera can be inferred from the Gaussian approximation involving the technical time resolution limit (δT_1) and the inherent photoelectron transit time dispersion (δT_2). Associated with the circular scan operation.

$$\delta T_1 \text{ (ps)} = \frac{100T}{\pi D \delta}$$

where T is the scan period (ns), D is the diameter (cm) of the circle and δ (lp/cm) is the dynamic spatial resolution. Substituting the values T = 3.3ns, D = 3cm and a realistic value of δ = 70 lp/cm under single-shot conditions, then δT_2 is 5ps. When a value of 2 - 3ps is taken for δT_1 for wavelengths somewhat away from the vicinity of the photosensitivity threshold of the cathode) then the instrumental function becomes approximately 6ps.

To check this prediction under experimental conditions, the camera was illuminated with pulses produced by a mode-locked, flashlamp-pumped rhodamine 700 dye laser. As can be seen from schematic of figure 8, seven pulses were selected from the 1us laser output train using a Pockels cell switch. As each pulse passed through the calibrated optical delay, two subpulses having a temporal separation of 66ps could be conveniently directed into the camera.

The pulse repetition period of just less than 3.3ns also meant that all seven streaked sub-pulse pairs could be recorded simultaneously. To ensure recordable intensity levels for these streaks while avoiding undue space charge effects (8), the gain of the microchannel plate intensifier was set to 10^4. At this level of gain, the background noise signal accumulated during the 10ms photographic recording exposure times was sufficiently low that it was not necessary to gate the forward bias voltage on to the

microchannel plate.

The disposition of the streaked laser pulses (without the optical calibration) on the circular scan is illustrated in figure 9(a) where the pulse selection has been deliberately timed during the evolutionary phase of the mode-locked train. To obtain more quantitative time resolution data, shorter pulses were selected later in the train where the steady-state had been established and a representative microdensitometer trace for one of the image pairs is included as figure 9(b). When the laser pulse durations which are typically 3 - 5ps at the operating wavelength of 760nm (22), are deconvolved from recorded streak duration of 5.7ps then the camera resolution is deduced to be 5ps. This is in good agreement with the predicted value for the instrumental function and clearly confirms that the Photochron IIC can perform to the required time resolution specification.

In addition to these single-shot streak tests, the camera was operated repetitively in conjunction with a mode-locked CW laser so that short-term phase stability could be assessed. Subpicosecond pulses (615nm) were produced at a 100 MHz repetition frequency by a passively mode-locked CW ring, rhodamine 6G dye laser (23). One of the two output beams was directed to the camera by way of a calibration glass disc as illustrated in figure 10 while the other triggered a tunnel-diode oscillator. This electrical output was then frequency tripled, filtered and amplified to provide the synchronised RF drive deflection to the streak tube. Because of the superpositioning of the streak images on the phosphor screen for this "Synchroscan" operation (12), there is no requirement for high electron gain in the intensifier section of the tube so a low gain setting 100 was selected.

For the purposes of providing an illustration of the circular scan and the display of streaked images, a small intensity

component of the pump argon ion laser as well as the dye subpulses were directed on to the input pinhole of the camera. A photographic recording of the resulting image is reproduced in figure 11(a) where the calibration delay between the ultrashort dye pulses is 57ps. The microdensitometer trace for such a pair of streak images in the absence of the background continuous illumination is included as figure 11(b) where it can be seen that the recorded streak duration is 4.7ps. Bearing in mind that subpicosecond pulsewidths are available from this test laser source (23), the main contribution to the recorded duration arises from the technical time resolution limit and to a lesser extent the photoelectron transit time dispersion and integrated jitter between the deflection voltage and the incidence of the laser pulses. Clearly this latter effect cannot be too significant because when account is taken of the expected photoelectron transit time dispersion (~2ps for 615nm wavelength and S20 photocathode) the implied technical time resolution limit is approximately 4ps. This is consistent with the expectation that under the conditions of repetitive streaking, the dynamic spatial resolution should exceed the corresponding value for single-shot operation.

It may therefore be concluded that phase drifts occurring during the recording periods (generally 1 - 5 seconds) are small and likely to be substantially less than 4ps for total supply RF powers of 15W. This result complements those of the single-shot experiement in that an instrumental time resolution of less than 6ps can be sustained over short term periods of several seconds.

5. CONCLUSION

The experimental data presented here confirm that the circular-scan Photochron IIC streak camera has a temporal resolution of better than 6ps and possesses good short term

stability of operation. For future applications, particularly those involving laser ranging, an electronic readout will be developed for full compatibility with telemetry.

It is envisaged that this readout will initially be a CCD camera placed external to the tube body and optically contacted to the existing faceplate via a fibre optic reducer. Although a circular array would appear to be the obvious form for the electronic readout it will probably turn out to be an impractical solution due to the difficulty involved in establishing optimum tube focus and scan characteristics. When in operation, a circular array would probably impose too severe a restraint on scan accuracy and alignment. The current development of large area two dimensional CCD arrays would appear in the future to offer the best solution to the problem. The placing of the electronic readout internally, as an integral part of the image tube, would appear to offer optimum performance by removing some of the loss coupling elements and some experiments will be carried out to ascertain the feasibility of this approach.

The detection of extremely low light-level signals involve a study of the various ways of improving the overall signal to noise ratio of the image tube. The usee of, for example, cooling of the photocathode and signal gating techniques will be investigated.

It has been demonstrated that a CSST can be constructed using metal and ceramic technology which should prove to be sufficiently rugged for spaceborne applications.

ACKNOWLEDGEMENT

The support of this work by ESTEC/ESA on Contract No. 5159/82/NL/HP(SC) is gratefully acknowledged.

6 REFERENCES

Abbreviations: ICHSP (P) - International Congress on High-Speed Photography (and Photonics)

(1) D E Smith, "Spaceborne Ranging System", Proc, 9th GEOP Conference, an International Symposium on the Application of Geodesy to Geodynamics, Dept of Geodetic Science, the Ohio State University, Report No 280, pp 59 - 64 (1978).

(2) H Lutz, W Krause and G Barthel, "High-Precision Two-Colour Spaceborne Laser Ranging System for Monitoring of Geodynamic Processes", Space 2000 (Edit: L G Napolitano) Amer Inst of Aeronautics and Astronautics, New York, p 236, 1983.

(3) C S Gardner, "Technique for Remotely Measuring Surface Pressure from a Satellite Using a Multicolour Laser Ranging System", Appl Opt Vol 18, pp 3184 - 3189, 1979.

(4) E K Zavoisky and S D Fanchenko, "Image-Convertor High-Speed Photography with 10^{-9} - 10^{-14}s Time Resolution", Appl Opt Vol 4, pp 1155 - 1167, 1965.

(5) R Hadland, K Helbrough and A E Huston, "Synchroscan - A Technique for the Photography of Repetitive Picosecond Pulses", Proc 11th ICHSP pp 107- 111, 1974.

(6) C E Johnson, S Nevin, J Bebris and J B Abshire, "Circular-Scan Streak Tube with Solid-State Readout", Appl Opt Vol 19, pp 3491 - 3495, 1980.

(7) P R Bird, D J Bradley and W Sibbett, "The Photochron II Streak Camera", Proc. 11th ICHSP, (London, Sept 1974) p 112.

(8) H Niu and W Sibbett "Theoretical Analysis of Space - Charge Effects in Photochron Streak Cameras", Rev Sci Instrum 52 (12), 1830 (1981).

(9) H Niu, W Sibbett and M R Baggs, "Theoretical Evaluation of the Temporal and Spatial Resolutions of Photochron Streak Image Tubes", Rev Sci Instrum, 53(5), 563 (1982).

(10) D J Bradley and W Sibbett, "Subpicosecond Chronoscopy", Appl Phys Lett, 27, 382 (1975).

(11) D J Bradley, S F Bryant, W Sibbett and J R Taylor, "Intensity-Dependent Time Resolution and Dynamic Range of Photochron Picosecond Streak Cameras", Rev Sci Instrum, 49 219 (1978).

(12) W Sibbett, "Synchroscan Streak Camera Systems", Proc 15th ICHSPP, SPIE 348 (San Diego 1982), p 15.

(13) M C Adams, W Sibbett and D J Bradley, "Linear Picosecond Electron-Optical Chronscopy at a Repetition Rate of 140 MHz", Opt Commun, 26 273 (1978).

(14) M C Adams, W Sibbett and D J Bradley "Electron-Optical Picosecond Streak Camera Operating at 140 MHz and 165 MHz Repetition Rates", Advances in Electronics and Electron Physics, 52, 265 (1979)

(15) P G May, W Sibbett, W E Sleat, J R Taylor and J P Willson, "Mode-Locked Ring C W Dye Laser Systems", Quantum Electronics and Electro-Optics, Edit P L Knight (John Wiley, 1983), p 33.

(16) W Sibbett, W E Sleat, J R Taylor and J P Willson, "Internally-Intensified Photochron II Streak Tube", Proc 15th ICHSPP (San Diego, August 1982) SPIE, 348, 217.

(17) P G May and W Sibbett, "Transient Stimulated Raman scattering of Femtosecond Laser Pulses", Appl Phys Lett 43, 624 (1983)

(18) D J Bradley, S F Bryant and W Sibbett, "Intensity-Dependent Time Resolution and Dynamic Range of Photochron Picosecond Streak Cameras - II, Linear Photoelectric Recording", Rev Sci Instrum, 51, 824 (1980).

(19) M Aslam, "An Investigation into Phosphor-Photocathode Cascade Screens for Use in Image Intensifiers", PhD Thesis, University of London, 1965.

(20) W Sibbett, W E Sleat and W Krause "Photochron Streak Tube for 300 MHz Circular Scan Operation", Proc 16th ICHSPP, Strasbourg 1984.

(21) W Sibbett, W E Sleat and W Krause, "Circular-scan Photochron Streak Camera for Spaceborne Laser Ranging Applications", Proc ESA Workshop on Space Laser Applications and Technology - ESA sp - 202, P171, 1984.

(22) W Sibbett and J R Taylor, "Passive Mode-locking in the Near Infrared", IEEE Quantum Electron, QE-20, 108, 1984.

(23) J P Willson, W Sibbett and W E Sleat, "Pulsewidth and Interpulse Jitter Measurement of a Passively Mode Locked ring C W Dye Laser", Opt Commun, 42, 208, 1982.

FIGURE CAPTIONS AND FIGURES

(1) Schematic of modular, externally-intensified single-shot streak camera.

(2) Comparison of deflection voltage profiles applied to single-shot and repetitively-operating (Synchroscan) streak cameras.

(3) Schematic of circular-scan Photochron IIA streak image tube.

(4) Scan distortion induced by amplitude and phase variations.

(5) Amplitude and Phase errors during one scan rotation.

(6) Circuit Diagram for 300 MHz oscillator.

(7) Photograph of Circular Sweep having 30 mm diameter.

(8) Experimental Set-up used in evaluation studies of single shot streak performance.

(9a) Uncalibrated streak images of seven "evolving" mode-locked dye laser pulses.

(9b) Microdensitometer trace for two "calibrated" streak images (reproduced in inset) of "steady state" dye laser pulses.

(10) Experimental set-up used for streak evaluation of repetively-operating camera.

(11a) Photograph of streak recording showing circular scan with superimposed ultra short laser pulse images.

(11b) Microdensitometer trace for two streaked images (reproduced in inset) associated with mode locked pulses

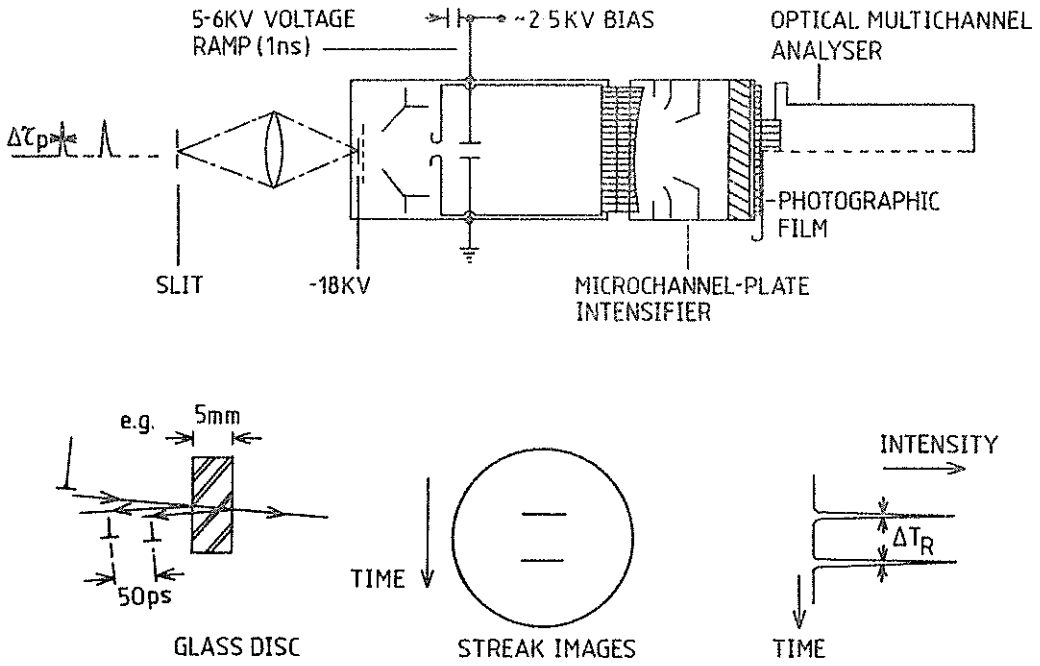

Figure (1)

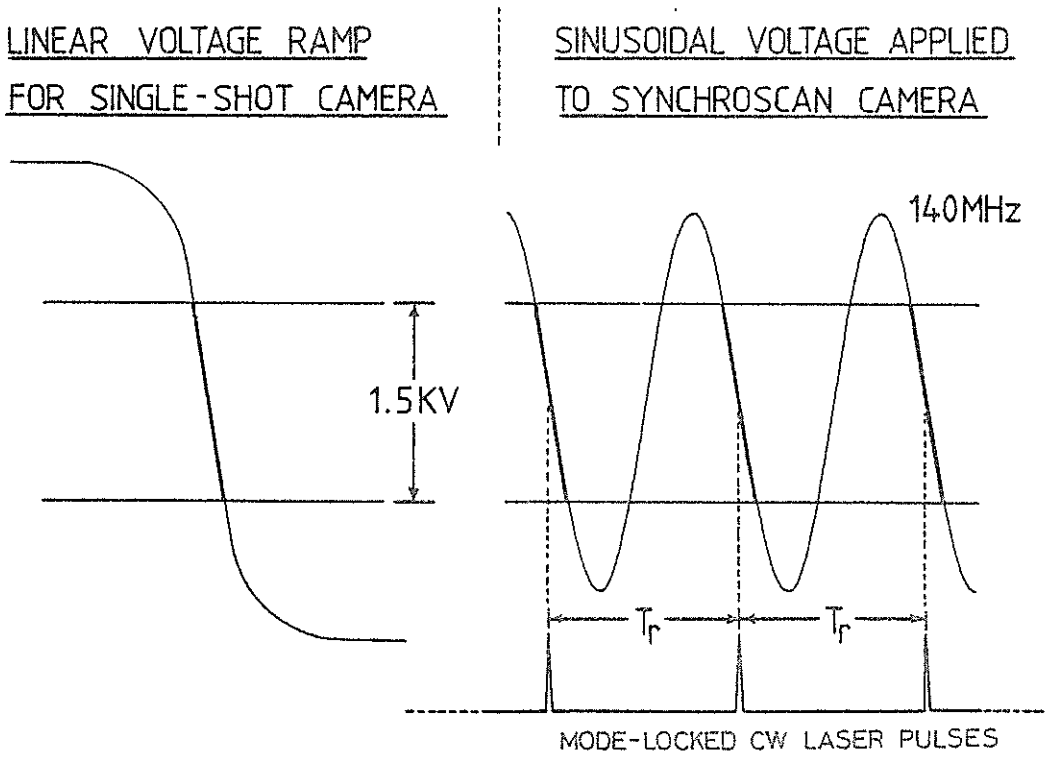

Figure (2)

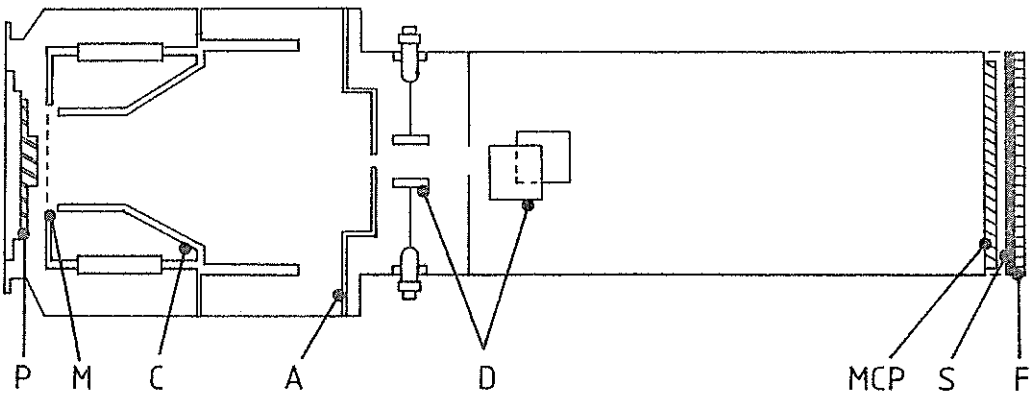

Figure (3)

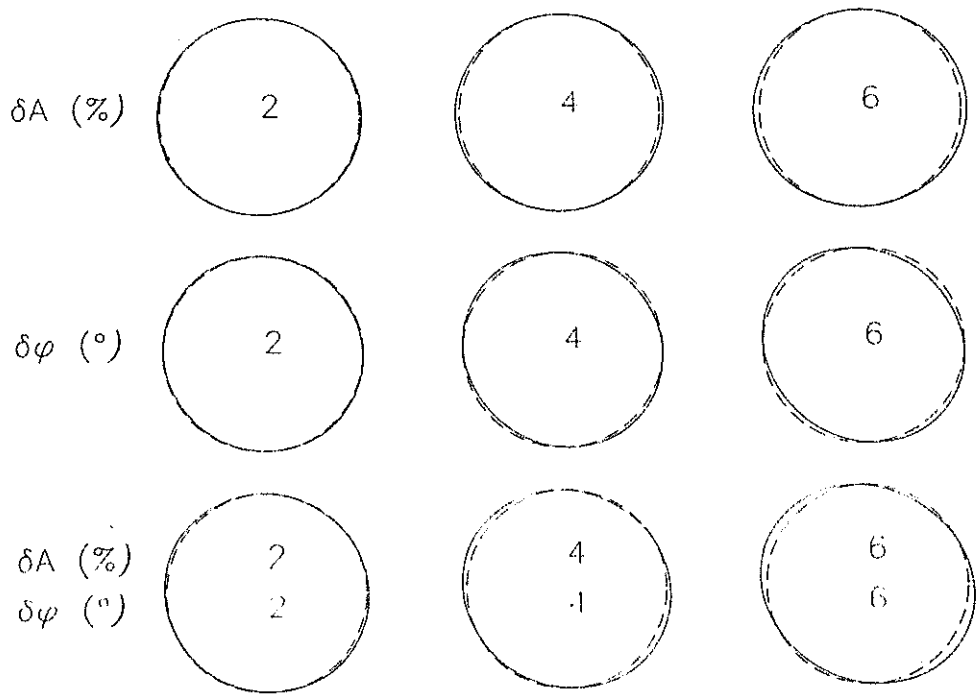

Figure (4)

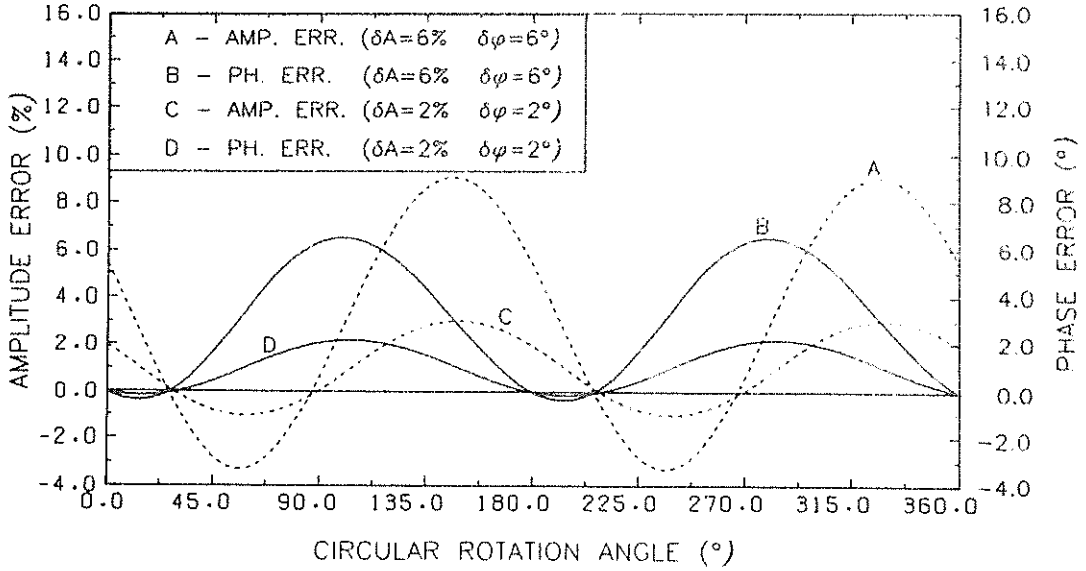

Figure (5)

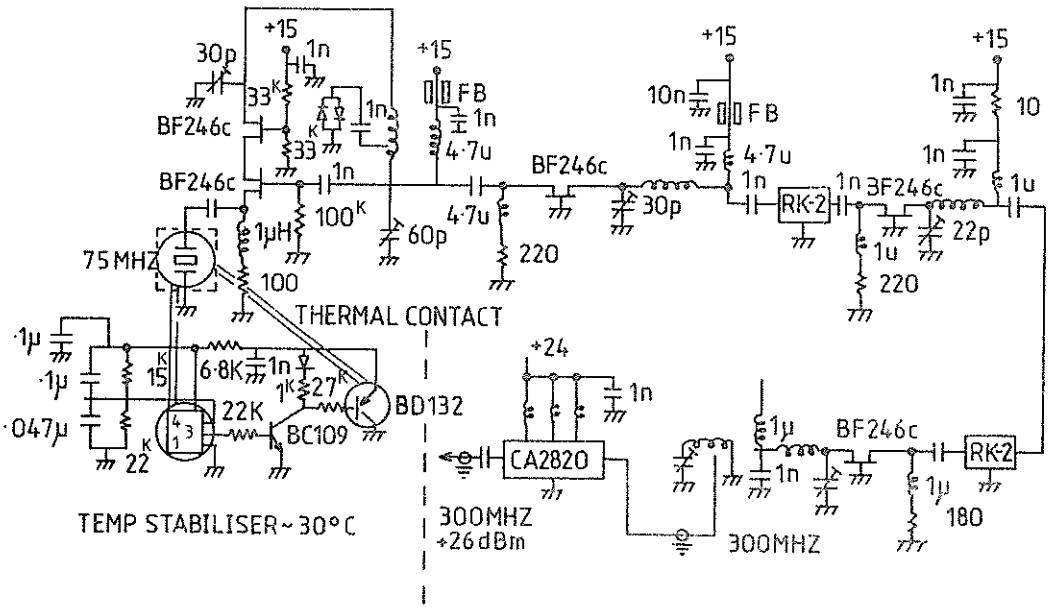

Figure (6)

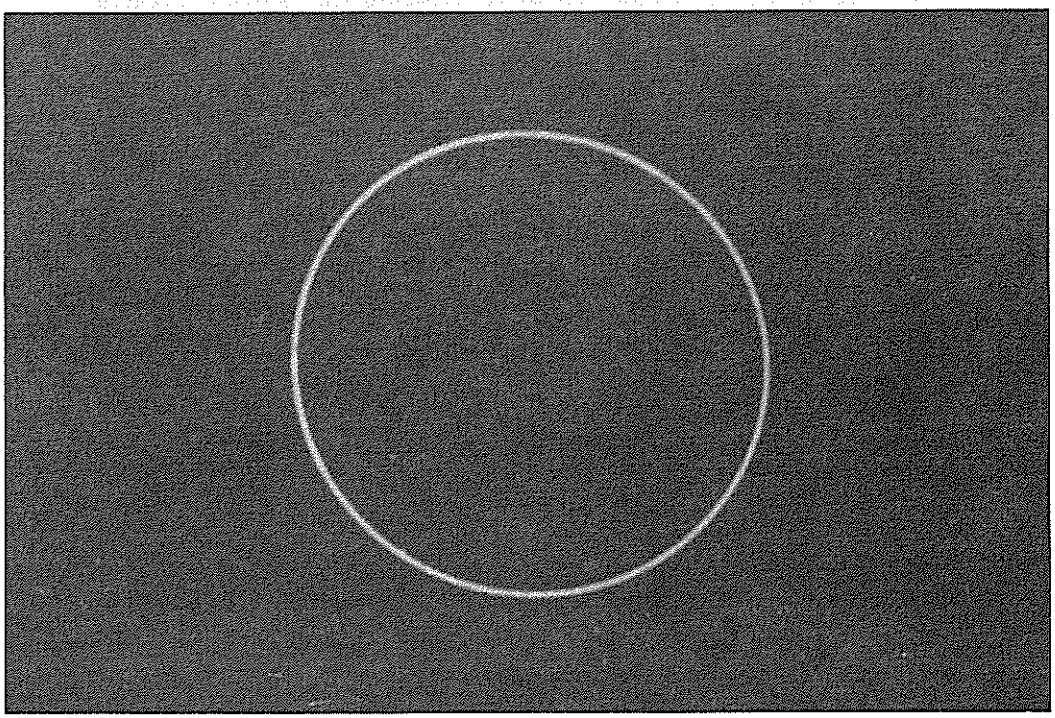

Figure 7

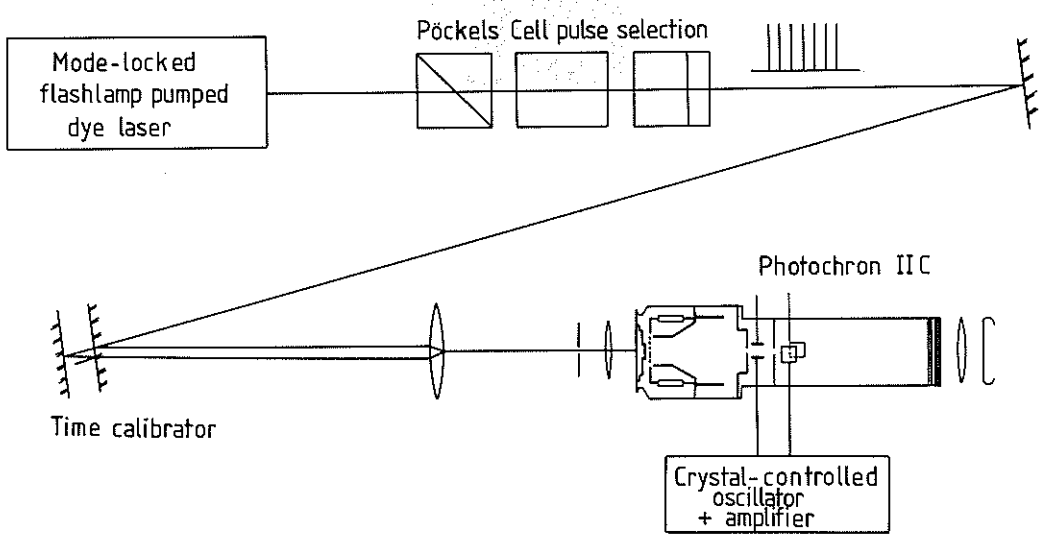

Figure 8

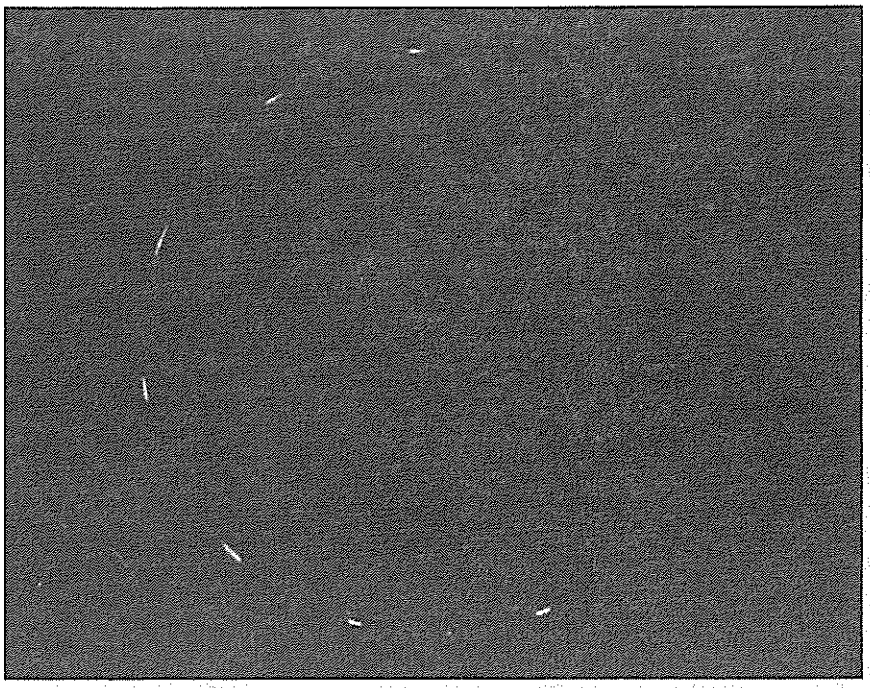

Figure 9a

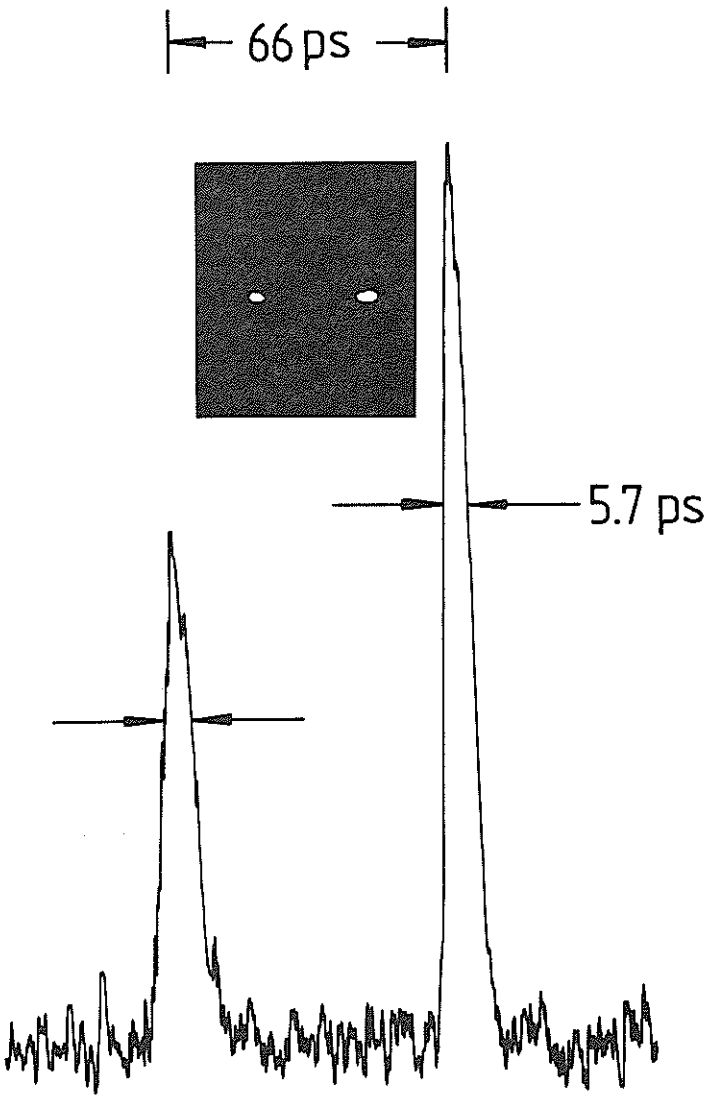

Figure 9b

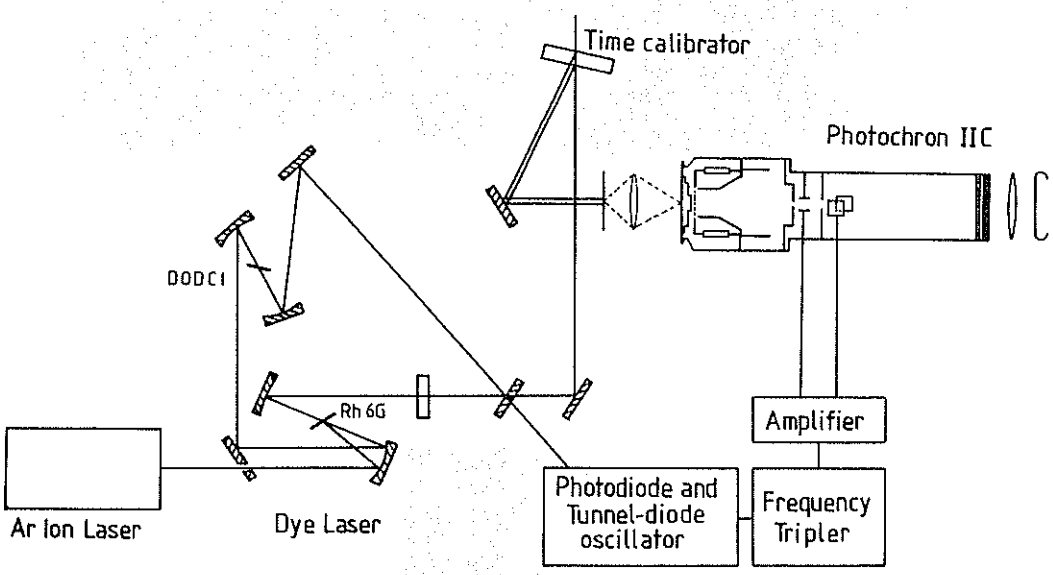
Time calibrator
Photochron IIC
DODCI
Rh 6G
Amplifier
Photodiode and
Tunnel-diode
oscillator
Frequency
Tripler
Ar Ion Laser
Dye Laser

Figure (10)

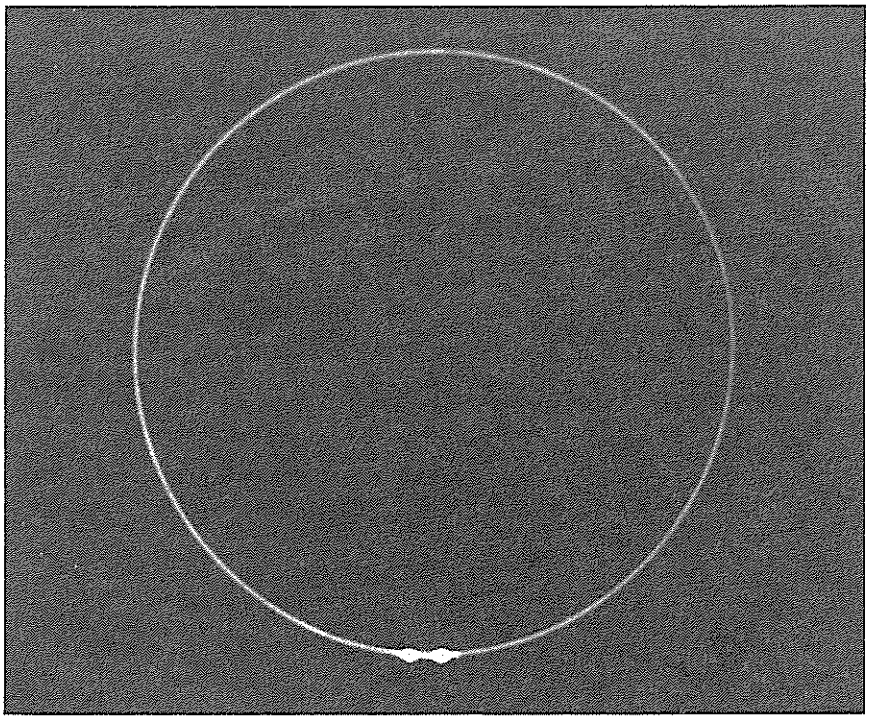

Figure 11a

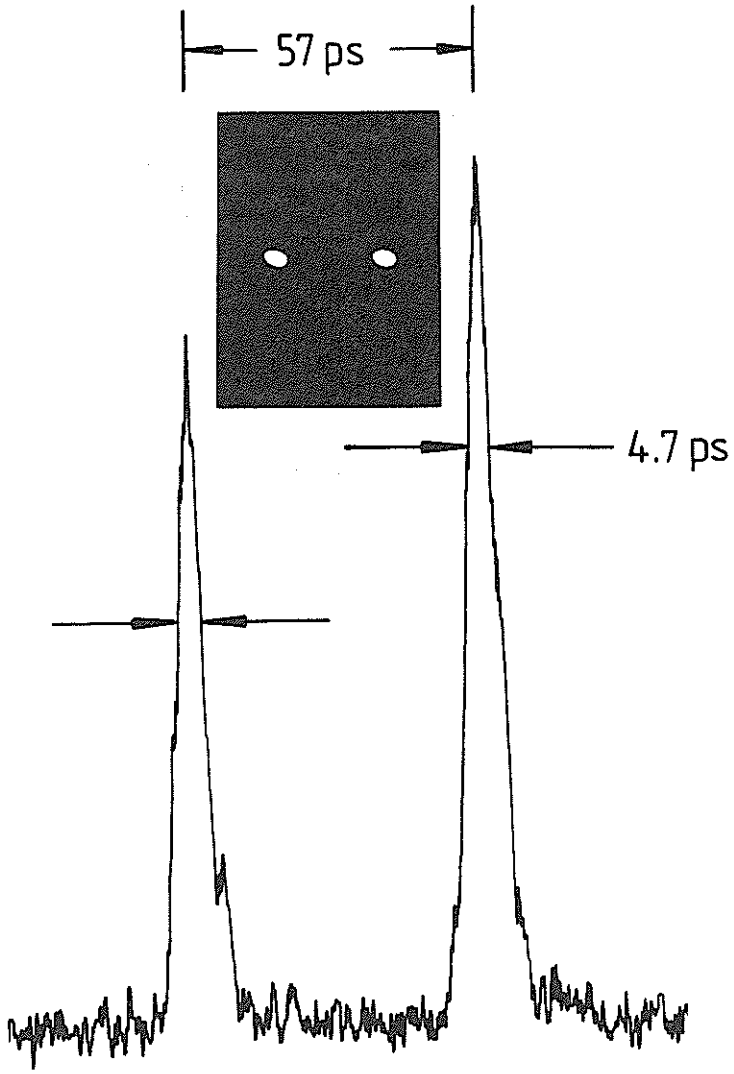

Figure 11b